On refined analysis of bifurcation buckling for the axially compressed circular cylinder

S. Opoka[a], W. Pietraszkiewicz[*,a]

[a] *Institute of Fluid-Flow Machinery, PASci, ul. Fiszera 14, 80-952 Gdańsk, Poland*

Abstract

We present extensive numerical results of bifurcation buckling analysis of the axially compressed circular cylinder. The analysis is based on the modified displacement version of the non–linear theory of thin elastic shells developed by Opoka and Pietraszkiewicz (2009, submitted to Int. J. Sol. Str.). To solve the buckling problem we apply the separation of variables and expansion of all fields into Fourier series in circumferential direction, with subsequent accurate calculations of eigenvalues of determinants of corresponding 8×8 complicated matrices. The numerical analysis of the buckling load is performed for the cylinders with length-to-diameter ratio in the range $(0.05, 60)$, with eight sets of incremental work–conjugate boundary conditions analogous to those used in the literature and partly summarized in the book by Yamaki (1984), and additionally with six sets of boundary conditions not discussed in the literature yet. The results allow us to formulate several important conclusions, such as: a) omission in the non-linear BVP small terms of the order of error introduced by the error of constitutive equations leads to overestimated buckling loads for long cylinders with clamped boundaries; b) for some relaxed boundary conditions the buckling load decreases for short cylinders with decrease of the cylinder length; c) the results for additional six sets of boundary conditions reveal existence of several new cases, in which by relaxing geometric boundary conditions the buckling load falls down to about one half of the classical value in a wide range of the cylinder length–to–diameter ratios.

Key words: Circular cylinder, Axial compression, Stability, Buckling, Boundary conditions, Non-linear theory

[*]Corresponding author. Phone: +48586995263; Fax: +48583416144; E-mail: pietrasz@imp.gda.pl

Email address: `szop@imp.gda.pl` (S. Opoka)

1. Introduction

Stability of the axially compressed thin, isotropic, elastic, circular cylinder belongs to the most discussed problems of structural mechanics. It was analysed in thousands of papers applying various shell models as well as various analytical and/or numerical techniques. Known results were partly summarised in several books, for example by Brush and Almroth (1975), Grigolyuk and Kabanov (1978), Yamaki (1984), and Tovstik and Smirnov (2001), where additional references to original papers and other books are given. The surveys by Simitses (1986), Knight and Starnes (1997), Mandal and Calladine (2000), Singer et al. (2002), and Arbocz and Starnes (2002) summarise more recent achievements in the field.

Experimental results reviewed by Weingarten et al. (1965), Babcock (1983), Yamaki (1984), Simitses (1986), and Singer et al. (2002) show wide scatter of experimental results and significant drop of the real buckling load of the axially compressed cylinder as compared to theoretical results. The main cause responsible for this discrepancy is usually associated with imperfections of shell geometry, boundary conditions, prebuckling states, material parameters, external loads etc. unavoidable in real cylindrical shell structures and real experimental conditions. As a result, the research in this area concentrates in the last decades primarily on measuring and modelling real imperfections of the cylinder and taking them into account in a more realistic engineering design, see for example Arbocz and Babcock (1969), Pircher et al. (2001), and Arbocz and Starnes (2002).

Yet, another important reason for differences mentioned above may be associated with the theoretical shell model used in the stability analysis. Already Donnell (1933) proposed simple non-linear shell equations for the cylinder using the simplest shallow shell approximation. This formulation in different but equivalent settings was used in many subsequent papers to calculate the buckling load of the axially compressed circular cylinder under various boundary conditions, see for example Kármán and Tsien (1941), Mushtari and Galimov (1957) , Vol'mir (1967), and Almroth (1966). More accurate but also more complex buckling equations for the cylinder follow from the equilibrium equations of shells of revolution proposed by Flügge (1932), see Yamaki (1984). Comparing square roots of characteristic polynomials resulting from the shell theories above, already Hoff and Brooklyn (1955) concluded that the Donnell stability equations are too inaccurate for the longer cylinders and when the circumferential wave number of buckling mode is less than four.

Yamaki (1984) compared the buckling load curves based on Donnell's and Flügge's stability equations for a wide range of length-to-radius ratio of the cylinder and for eight sets of incremental boundary conditions, using the membrane prebuckling state. He found that for the most sets of his boundary conditions the results following from the Donnell stability equations are approximately valid only for cylinders with intermediate lengths indeed. With the increase in the cylinder length the buckling loads following from the Flügge stability equations took considerably smaller values than those following from the Donnell ones. Several non-linear models of thin shells undergoing moderate deflections were proposed by Mushtari and Galimov (1957), Sanders (1963), Koiter (1960), and Pietraszkiewicz (1977). The stability equations for the cylinder based on these models are more complex than the Donnell ones, but simpler than the ones of Flügge.

Even more complex stability equations were developed by Koiter (1967), Budiansky (1968), Stumpf (1984), and Pietraszkiewicz (1984, 1993). For the axially compressed cylinder, Dym (1973) concluded that the Koiter-Budiansky stability equations give results in good agreement with those of Flügge. Thus, it seems justifiable to consider the stability equations based on the Flügge shell equations as a reference formulation for the buckling problems of the axially compressed cylinder.

In all the analyses on buckling of axially compressed circular cylinder we are aware of, the incremental boundary conditions of the buckling problem were not carefully derived but were rather assumed in the form analogous to the one used in the simple versions of non–linear theory of shells. But already Pietraszkiewicz and Szwabowicz (1981) noted that in the non-linear displacement BVP for thin shells the boundary rotation should be expressed by a scalar function of displacement derivatives, and only this allows one to formulate correctly the work-conjugate sets of geometric and static boundary conditions. The sets of work-conjugate incremental boundary conditions should then be derived by consistent linearization of the incremental displacements about the equilibrium prebuckling state.

In this paper we perform the refined numerical analysis of bifurcation buckling for the axially compressed circular cylinder. The analysis is based on the modified version of the geometrically non-linear theory of thin, isotropic, elastic shells expressed in terms of displacements as the only independent field variables, which has been developed in the accompanying paper by Opoka and Pietraszkiewicz (2009). In that paper we have formulated alternative work-conjugate sets of geometric and static boundary conditions introducing a new boundary function α

rational in terms of displacement derivatives. Using this version of shell theory we are able here to refine for this buckling problem the results summarized, for example, by Yamaki (1984) in three main aspects:

1. In our formulation the non–linear BVP for a thin shell and the corresponding shell buckling problem (SBP) are generated automatically by the computer program written within the symbolic language of MATHEMATICA. These problems for shells are formulated without using any kind of approximations, apart of those following from the underlying principle of virtual work postulated for the shell reference surface. Such an approach leads to extremely complex shell relations available only in the computer memory with many supposedly small and mostly unimportant terms. But this allows one to always account for those a few small terms in the buckling shell problem which may be critical for finding the correct buckling load of the axially compressed circular cylinder.
2. In our formulation the incremental boundary conditions of the SBP are derived by direct linearization of the correct work-conjugate sets of the non–linear geometric and static boundary conditions about the prebuckling equilibrium state. Our buckling loads for the axially compressed circular cylinder, calculated using those correctly linearized incremental boundary conditions, allow one either to confirm the results published elsewhere, or to refine those which seem to be questionable. In particular, this allows us to clarify the behaviour of the buckling loads for short cylinders when their lengths are decreasing.
3. Additionally to eight sets of incremental work–conjugate boundary conditions analogous to those discussed in the literature and summarized by Yamaki (1984), we analyse also six other sets of boundary conditions not discussed elsewhere. Among them are cylinders with boundary conditions S5, S6, and S7. It is shown in particular that the buckling load of the axially compressed cylinder with these boundary conditions also falls down to about one half of the classical value in the range of experimental cylinder lengths, similarly as in the cases S3 and S4 (in our nomenclature) discussed by Yamaki (1984) and S4 also by Simmonds and Danielson (1970).

The present paper is organized as follows. In Section 2 we remind some notation for the axially compressed circular cylinder, the prebuckling equilibrium state used here, as well as the homogeneous shell buckling equations with corresponding work-conjugate sets of boundary conditions of the displacement buckling problem. More detailed derivation of the relations of Section 2 is given in

Appendix, where the results of the paper by Opoka and Pietraszkiewicz (2009) have been used. The solution method applied in our buckling problem, based on the separation of variables with subsequent expansion of all fields into Fourier series in the circumferential coordinate, is presented in Section 3. We also discuss there some details on automatic generation of determinants of 8×8 matrices for each circumferential wave number of buckling mode n by symbolic language of Mathematica, on numerical analysis of eigenvalues of the determinants, and on step sizes used in different ranges of the length–to–diameter ratio to assure appropriate accuracy of the results.

In Section 4 we present extensive numerical results of the refined analysis of bifurcation buckling for the axially compressed circular cylinder under fourteen different, carefully derived work–conjugate sets of boundary conditions. For each set of the boundary conditions our results are given by one graph for the length–to–diameter ratios in the range $(0.05, 60)$. This proves versatility of the analytic–numerical method used here; to calculate such a detailed one graph using existing finite element codes would require enormous computational efforts without possibility to correctly model various cases of non–linear work–conjugate boundary conditions. The numerical results presented here are used to discuss some aspects of stability behaviour of the axially compressed cylinder. In particular, in Subsection 4.1 we show that omission in the non–linear BVP of all small terms of the order of error introduced by the constitutive equations leads to overestimated buckling loads for long cylinders. In Subsection 4.2 we show that for the cylinders with eight sets of work–conjugate boundary conditions our results practically coincide with or are slightly lower than those given by Yamaki (1984). However, for cylinders with boundary conditions C4 and S4 we obtain different asymptotic behaviour of the critical curves for short cylinders: with decrease of the cylinder length the critical curves by Yamaki (1984) increase, while our results show decrease of those curves. This behaviour of the critical curves, noted already by Koiter (1967) and Simmonds and Danielson (1970), can be explained by using in our analysis the correct incremental work-conjugate boundary conditions.

In Subsection 4.3 we use our results for six additional sets of work–conjugate boundary conditions to analyze in more detail the effect on the buckling loads of exchange of one geometric boundary condition for the corresponding work–conjugate static one. From the literature we know that by relaxing the incremental boundary constraint $v = 0$ for circumferential displacements the buckling load falls down to about one half of the classical value in the wide range of cylinder lengths. But we have discovered several cases not mentioned in the literature in which by relaxing incremental boundary constraint $w = 0$ for radial displacements, or $w' = 0$ for rotations the buckling load falls down to about one half of the classical value as well. This confirms once more the importance of boundary conditions for scatter of the experimental buckling loads observed in this problem, because the fixation of cylinder boundaries is newer complete in the testing setups.

In Subsection 4.4 we compare the behaviour of axially compressed long cylinder and Euler column of the same length.

When the buckling load is exceeded, a dynamic process takes place in the cylinder leading either to its damage or to the transient motion with subsequent decaying vibrations about a new equilibrium state far from the primary equilibrium path. The post-buckling behaviour of shells was discussed theoretically and numerically in many papers and books, see for example Riks (1998), Chróścielewski et al. (2004), Wriggers (2008) or Amabili (2008) and references given there. But the post-buckling behaviour of the cylinder cannot influence the value of the buckling load itself, which is the only goal of the present paper.

2. Modified displacement stability equations and boundary conditions for the axially compressed circular cylinder

The reference surface $\mathscr{M}$ of the circular cylinder with radius R, length L, and thickness h is loaded by the compressive axial force component uniformly distributed on both boundaries perpendicular to cylinder's generators. The cylindrical surface is parameterized by non-dimensional coordinates $(\phi, x = z/R)$. The independent field variables of the BVP are displacements of the reference surface. The non-dimensional incremental displacements $u(\phi, x)$, $v(\phi, x)$ and $w(\phi, x)$ denote, respectively, the axial, circumferential and radial components of the incremental displacement vector, see Fig. 1.

The modified displacement version of the non-linear theory of thin elastic shells used here has been presented in detail in the accompanying paper by Opoka and Pietraszkiewicz (2009). The reader is asked to consult that paper in order to fully understand notation as well as formulation of the BVP and derivation of corresponding SBP which are used here for the axially compressed circular cylinder. In Appendix we present more detailed description of cylindrical shell geometry and definitions of various non-dimensional fields of the BVP. We also describe there the main steps of generating the BVP and the SBP using the package *Shell-BVP.m* written in Mathematica.

Under compression by the axial force components $N_\nu^* = -\frac{2\rho}{\epsilon}$ uniformly distributed along both boundaries the cylinder becomes shorter and is assumed to

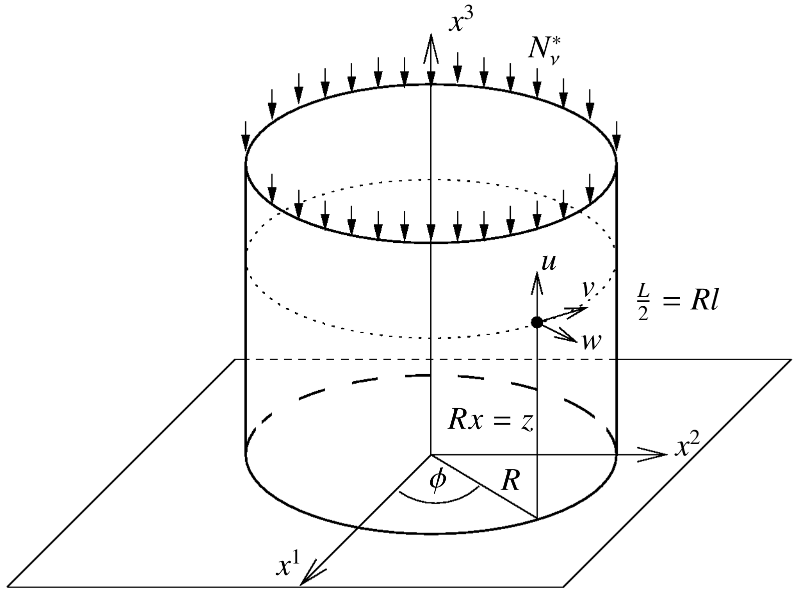

Figure 1: The parameterized upper-half of the cylindrical surface.

homogeneously expand in the radial direction. The prebuckling equilibrium solution for the cylinder has been found in the Appendix to be

$$
\begin{aligned}
u_0(\phi, x) &= Ux = -2\epsilon\rho(1 + 3\epsilon\rho)x \;, \\
v_0(\phi, x) &= 0 \;, \\
w_0(\phi, x) &= W = 2\epsilon\nu\rho[1 + (2 - \nu)\epsilon\rho] \;,
\end{aligned}
\tag{1}
$$

where ν denotes Poisson's ratio, the small parameter of the theory ϵ is defined as $\epsilon^2 = h^2/[12(1-\nu^2)R^2]$, and ρ denotes the load parameter. The value $\rho = 1$ is usually called the classical value of the buckling load and corresponds to the buckling stress $\sigma_{cl} = 2\epsilon Eh$.

The assumed prebuckling displacements in (1) are relatively small, because they are proportional to the small parameter ϵ. This allows us to identify geometry of the deformed prebuckling state with that of the initial state of the cylinder. Using the linear constitutive equations and the non-linear kinematic relations, we can show that the prebuckling solution (1) defines approximately the membrane prebuckling state with only one internal stress resultant $N_x = -\frac{2\rho}{\epsilon}$.

The displacement buckling problem of the axially compressed elastic cylinder, which is derived in Appendix from the exact BVP of Opoka and Pietraszkiewicz (2009) under assumption of the membrane prebuckling state (1), consists of three homogeneous linear PDEs with constant coefficients with regard to incremental displacements u, v, w (see A-23)

$$
\begin{aligned}
&A_1 w^{\bullet\bullet\bullet} + A_2 w''^{\bullet} + A_3 u'^{\bullet} + A_4 v'' + A_5 v^{\bullet\bullet} + A_6 w^{\bullet} = 0 \ , \\
&B_1 (w'^{\bullet\bullet} + \nu w''') + B_2 u'' + B_3 u^{\bullet\bullet} + B_4 [(1+\nu) v'^{\bullet} + 2\nu w'] = 0 \ , \\
&C_1 (w'''' + 2 w''^{\bullet\bullet} + w^{\bullet\bullet\bullet\bullet}) + C_2 (u'^{\bullet\bullet} + \nu u''') + C_3 v''^{\bullet} + C_4 v^{\bullet\bullet\bullet} + C_5 w'' \\
&\ + C_6 w^{\bullet\bullet} + C_7 u' + C_8 v^{\bullet} + C_9 w = 0 \ ,
\end{aligned}
\tag{2}
$$

and four homogeneous work–conjugate boundary conditions defined at $x = \pm l = \pm\frac{L}{2R}$ to be (see A-24)

$$
\begin{aligned}
&d_1 \equiv D_1 w'' + D_2 u' + D_3 (v^{\bullet} + w) = 0 && \text{or} \quad u = 0 \ , \\
&d_2 \equiv E_1 w'^{\bullet} + E_2 u^{\bullet} + E_3 v' = 0 && \text{or} \quad v = 0 \ , \\
&d_3 \equiv F_1 [w''' + (2-\nu) w'^{\bullet\bullet}] + F_2 (u^{\bullet\bullet} + \nu u'') + F_3 v'^{\bullet} + F_4 w' = 0 && \text{or} \quad w = 0 \ , \\
&d_4 \equiv G_1 (w'' + \nu w^{\bullet\bullet}) + G_2 v^{\bullet} + G_3 u' + G_4 w = 0 && \text{or} \quad w' = 0 \ ,
\end{aligned}
\tag{3}
$$

where $\frac{\partial()}{\partial x} = ()'$, $\frac{\partial()}{\partial \phi} = ()^{\bullet}$. The coefficients appearing in (2) and (3) are defined in (A-25) and (A-26). More information about the equilibrium BVP, the assumed prebuckling state and the derivation of the shell buckling problem (2) and (3) can be found in Appendix.

The numerical results presented in this paper have been calculated using the stability equations (2) with different sets of boundary conditions (3) defined in Table 1. Considering only the constraints imposed on incremental displacements

Table 1: Nomenclature for different sets of boundary conditions

C–family					S–family				
C1:	$u=0$	$v=0$	$w=0$	$w'=0$	S1:	$u=0$	$v=0$	$w=0$	$d_4=0$
C2:	$d_1=0$	$v=0$	$w=0$	$w'=0$	S2:	$d_1=0$	$v=0$	$w=0$	$d_4=0$
C3:	$u=0$	$d_2=0$	$w=0$	$w'=0$	S3:	$u=0$	$d_2=0$	$w=0$	$d_4=0$
C4:	$d_1=0$	$d_2=0$	$w=0$	$w'=0$	S4:	$d_1=0$	$d_2=0$	$w=0$	$d_4=0$
C5:	$u=0$	$v=0$	$d_3=0$	$w'=0$	S5:	$u=0$	$v=0$	$d_3=0$	$d_4=0$
C6:	$d_1=0$	$v=0$	$d_3=0$	$w'=0$	S6:	$d_1=0$	$v=0$	$d_3=0$	$d_4=0$
C7:	$u=0$	$d_2=0$	$d_3=0$	$w'=0$	S7:	$u=0$	$d_2=0$	$d_3=0$	$d_4=0$
C8:	$d_1=0$	$d_2=0$	$d_3=0$	$w'=0$	S8:	$d_1=0$	$d_2=0$	$d_3=0$	$d_4=0$

u, v, and w (corresponding static boundary conditions differ in the literature due to different model assumptions used in deriving appropriate shell BVPs), the nomenclature in Table 1 is the same as in Sobel (1964), Bushnell (1981), and Tovstik and Smirnov (2001). In particular, this nomenclature is applied here also to the results given by Yamaki (1984), where somewhat different classification of the boundary conditions was used. In our nomenclature the classical simply supported and clamped boundary conditions are denoted, respectively, as S2 and C1.

In our numerical analysis the discussion of buckling of the compressed cylinder with boundary conditions C8 and S8 have been omitted. In these two cases the cylinder is globally kinematically unstable and under compression a rigid body motion may appear much earlier than the shell buckling phenomenon.

3. Solution method

Assuming the separation of variables and expanding all fields into Fourier series in the circumferential coordinate ϕ, we obtain the infinite series of sets of equations which define the general solution of the buckling problem (2) and (3). Because the stability equations are linear PDEs, different harmonics can be uncoupled and we can divide the whole problem into simple cases: each for the integer–valued wave number n. Thus, the solution of (2) and (3) for each n can be postulated in the following form:

$$u(\phi,x) = Ue^{px}\cos(n\phi)\ , \quad v(\phi,x) = Ve^{px}\sin(n\phi)\ , \quad w(\phi,x) = We^{px}\cos(n\phi)\ . \tag{4}$$

Substituting (4) into (2) we obtain the set of three algebraic equations with regard to the constants U, V, W. If we solve these equations with respect to, for example, the constant U we obtain two relations

$$V = V(\nu,\epsilon,n,\rho;p_j,U)\ , \quad W = W(\nu,\epsilon,n,\rho;p_j,U)\ , \tag{5}$$

and the polynomial characteristic equation having the roots p_j. For each root p_j the postulated forms (4) together with (5) are special solutions of the stability equations (2). Due to the superposition principle, the general solution in the coordinate x is the sum of all these special solutions.

The structure of the stability equations (2) causes that for $n \geq 1$ the polynomial characteristic equation has eight non-zero roots p_j which equal the number of the available boundary conditions. But for $n = 0$ the polynomial characteristic equation has only four non-zero roots, contrary to six boundary conditions available (the second static and geometric boundary conditions are identically satisfied for $n = 0$). To avoid this incompatibility we need to specify at least two additional constants in the solution when $n = 0$. To generate these constants we assume that for $n = 0$ the displacements are polynomials in the x variable, i.e. $\sum_{k=1}^{3} A_k x^k$. Substituting this assumed solution into stability equations (2) and solving the resulting algebraic problem one obtains that u is a linear function of x, v is zero, and w is constant. This additional solution when $n = 0$ is added to the general solution. As a result, the solution of the buckling problem (2) and (3) for any n takes the modified form

$$
\begin{aligned}
u(\phi, x) &= \sum_j U_j e^{p_j x} \cos(n\phi) - \frac{1-\epsilon(6-8\nu)\rho+\epsilon^2[1-\nu^2-2(3+16\nu-8\nu^2)\rho^2]}{\nu[1-2\epsilon\rho(4-3\nu+3\epsilon(6-\nu)\nu\rho)]} S\, x + Z\ , \\
v(\phi, x) &= \sum_j V(\nu, \epsilon, n, \rho; p_j, U_j) e^{p_j x} \sin(n\phi)\ , \\
w(\phi, x) &= \sum_j W(\nu, \epsilon, n, \rho; p_j, U_j) e^{p_j x} \cos(n\phi) + S\ ,
\end{aligned}
\tag{6}
$$

where non-zero A_k's are named S and Z, respectively.

The solution (6) is then substituted into different sets of incremental homogeneous boundary conditions (3) defined at $x = \pm l$, see Table 1. In each case the resulting algebraic equations describe linear relations between still undetermined constants U_j (and S, Z for $n = 0$). Coefficients of these constants in those relations form a 8×8 matrix (6×6 matrix) for $n \geq 1$ ($n = 0$). The non-trivial buckling load ρ_{crit} exists if the determinant of the matrix vanishes.

In the numerical analysis we have substituted $\frac{3}{10}$ for Poisson's ratio and $\frac{1}{100}$ for $\frac{h}{R}$ into the resulting matrices. Then, we have generated using Mathematica the symbolic expression for the determinant of the matrix for each positive integer value of n. These expressions are extremely complex and are explicitly available only in the computer memory. Assuming that the determinant is the continuous function of ρ, for any fixed value of $l = L/2R$ the eigenvalues ρ_{crit} of this function have been detected as follows. For the fixed value of l, the value of determinant has been probed from $\rho = 0$ to $\rho = 1$ with the step $\Delta\rho$. If the determinant has changed its sign between ρ_i and ρ_{i+1} then ρ_i (the smaller value) has been taken as the value of the buckling load. If the determinant has numerically vanished at ρ_i then ρ_i has been taken as the value of the buckling load. If for a particular l there have been several values of ρ changing the sign of the determinant on the line $\rho \in (0, 1]$, then the smallest value of such ρ has been interpreted as the value of the buckling load.

For each probed value of ρ_i, the determinant has been calculated using a numerical-precision control feature of MATHEMATICA. It means that the program itself has performed internal intermediate calculations with a much higher precision in order to obtain the numerical value of the determinant with the prescribed accuracy. In our calculations the accuracy was set to 15 digits. The program ensured that 15 digits after decimal point were correct, and the absolute value of the determinant less than 10^{-15} was interpretted as numerical zero.

Some difficulty in this procedure has been to properly determine the step size $\Delta\rho$. Too large step size could cause omission of some zeros due to possible faster sign changes of the probed determinant. The prescribed value of $\Delta\rho = 0.001$ has been assumed to be sufficiently small for detecting all sign changes of the determinant.

The numerical procedure has been repeated with the following steps: $\Delta l = 0.005$, $\Delta l = 0.05$, $\Delta l = 0.1$ and $\Delta l = 0.5$ in the ranges $l \in (0.05, 0.2]$, $l \in (0.2, 1]$, $l \in (1, 10]$ and $l \in (10, 60]$, respectively. The computations have been performed for all integer values of n varying from 0 to 14. Each buckling load curve given in Section 4 represents over 230 buckling loads of the compressed cylinder with different length-to-diameter ratio. To obtain comparable results by any of FEM computer codes one would need to analyse over $14x230 = 3220$(!) examples of the cylinder, each with different boundary conditions and different length-to-diameter ratio, which would require an enormous unrealistic computational work. Additionally, the 3-f shell model itself requires to use finite elements with translations and their first and second surface gradients as dof‘s at the element nodes as well as C^1 interelement continuity. Such elements are very complex and numerically inefficient. These remarks were the main reasons why in this paper we have not used the numerical analyses based on the finite element method.

4. Numerical results

The numerical results indicating buckling load curves for the axially compressed perfect cylinder with different sets of boundary conditions (see Table 1) are given in Figures 2–5. In the Figures the value $\rho = 1$ corresponds to the classical value of the buckling load and the results are positioned with respect to the horizontal, logarithmic axis of the non–dimensional cylinder length $l = \frac{L}{2R}$. In the analysis we have divided the range of cylinder's length into three following intervals: if $l \leq 0.1$ then the cylinder is regarded as short; the practical cylinder lengths (PCL) cover the interval $l \in (0.1, 20)$; long cylinders are those for which $l \geq 20$. Within the interval of PCL we introduce experimental cylinder lengths (ECL) when $l \in (0.2, 5)$. The interval of ECL covers the range of lengths of the axially loaded real cylinders used in experiments. Among all fourteen configurations of boundary conditions discussed here we identify C1, C2 and S1, S2 as the practical sets of boundary conditions, because they seem to be the best approximations of the real boundary conditions.

Generally, the fourteen types of boundary conditions (Fig. 2-5) can be divided into three groups. In cases S1, C1, C3 and C5 the buckling load takes generally high values which practically coincide when $l \in (0.7, 60)$. In the second group S2, C2, C4, C6 and C7 of boundary conditions the buckling load takes intermediate values and the curves are choppy. The results for this group again practically coincide when $l \in (2.5, 60)$. For the last group of boundary conditions S3, S4, S5, S6 and S7 the buckling load ρ assumes about one half of the classical value for PCL and the results practically coincide only when $l \in (0.1, 20)$.

Interpretation of the numerical results is splitted into four parts.

4.1. Influence of different approximations in the derivation of the stability problem

The procedure used in the derivation of the complete stability equations (2) and the simplified ones (A-27) has been the same. In particular, the same approximate prebuckling state was assumed and full non-linear kinematic relations were used. Therefore, the only difference in derivation of stability equations (2) and (A-27) was the starting point: the equilibrium equations. The complete stability equations (2) were derived from the two-dimensionally exact equilibrium equations, whereas the simplified ones (A-27) were derived using the equilibrium equations with only underlined terms (Opoka and Pietraszkiewicz, 2009, eq. (21)), where terms of the order of error introduced by the constitutive equations were omitted. Thus, differences between the results can be directly attributed to elimination of supposedly small terms from the equilibrium equations, because we have used the same exact clamped boundary condition C1.

The numerical results obtained from the complete stability problem (C1 curve) and from the simplified one ($C1_S$ curve) are shown in Figure 2. For ECL, differences between the results are small, but with increase of the cylinder length the simplified stability equations lead to more and more overestimated results. This reflects a similar conclusion suggested by Buchwald (1967, 1968) within the linear first-approximation theory of thin elastic shells. He found that some simplified versions of the linear shell equations for the cylinder, obtained by omitting some supposedly small terms, led to incorrect solution for long cylinders. Hence, some supposedly small terms are, in fact, important and cannot be omitted for long cylinders.

If in the simplified equilibrium equations (Opoka and Pietraszkiewicz, 2009, eq. (21)), where only the underlined terms are considered, we eliminate M^{α}_{β} by the linear constitutive equation and introduce the simplified kinematic relations (Brush and Almroth, 1975, eq. (5.7)), then using the perturbation technique we arrive at the simplified stability equations equivalent to the Donnell ones. Comparing $\rho = 1$ (obtained using the Donnell stability equations for the C1 case) with $C1_S$ curve we note that the difference is small for PCL and the simplification of kinematic relations becomes important again only for long cylinders. Because of these differences, we have decided to perform the remaining calculations leading to corresponding critical curves presented in the Figures 2–5 using the complete stability problem (2) and (3).

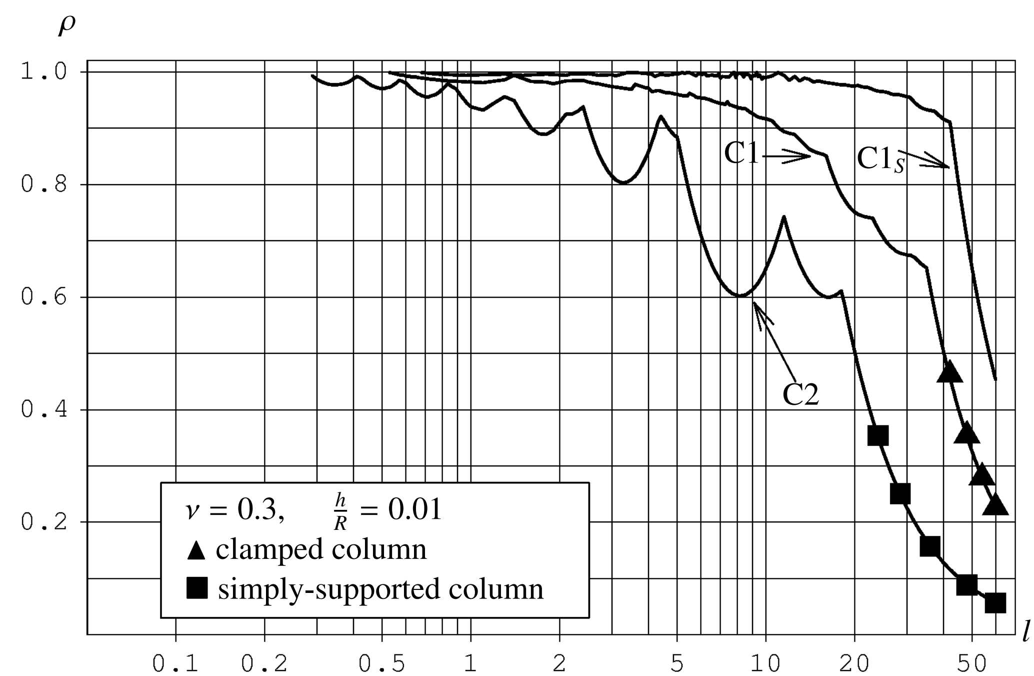

Figure 2: The buckling load of axially compressed perfect cylinder for boundary conditions C1 and C2.

4.2. Comparison of our results with ones given in the literature

The bifurcation buckling of the axially compressed circular cylindrical shell with eight sets of boundary conditions was investigated by Yamaki (1984) using the stability equations based on the Donnell and Flügge non-linear shell equations together with corresponding incremental boundary conditions. These stability problems were derived assuming the membrane prebuckling state. It was noted that the results based on the Donnell equations, as compared to the Flügge ones, give more and more overestimated results with the increase of the cylinder length. We have compared our results with eight ones available in Yamaki (1984) based on the Flügge stability theory. The results calculated by Yamaki (1984) represented by dotted curves are shown in Figures 3 and 4.

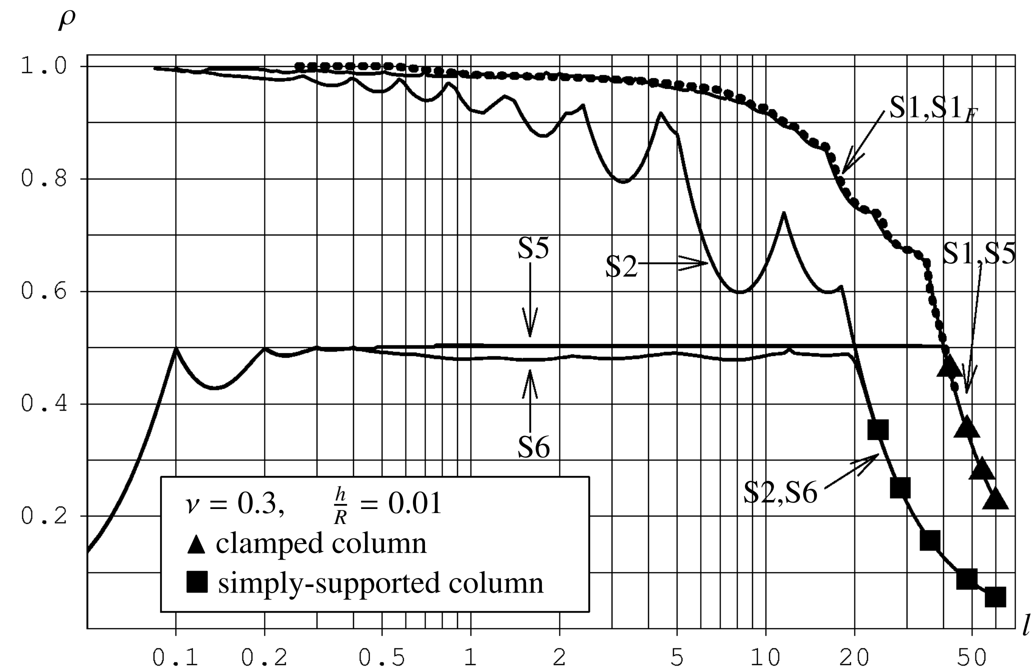

Figure 3: The buckling load of axially compressed perfect cylinder for boundary conditions S1, S2, S5 and S6.

For the boundary conditions C1, C2, C3, S1, S2 and S3 in the range of PCL and long cylinders our results practically coincide or are slightly lower than those of Yamaki. Therefore the Yamaki results for these cases are not shown in the Figures 3 and 4, except for S1 case in Figure 3 given as an example. Because of good overall agreement between the corresponding curves, the Flügge stability equations with his boundary conditions could be preferred as the simpler ones.

However, for short cylinders with boundary conditions S4 and C4 the completely different type of behaviour of the critical curves is noted between the both

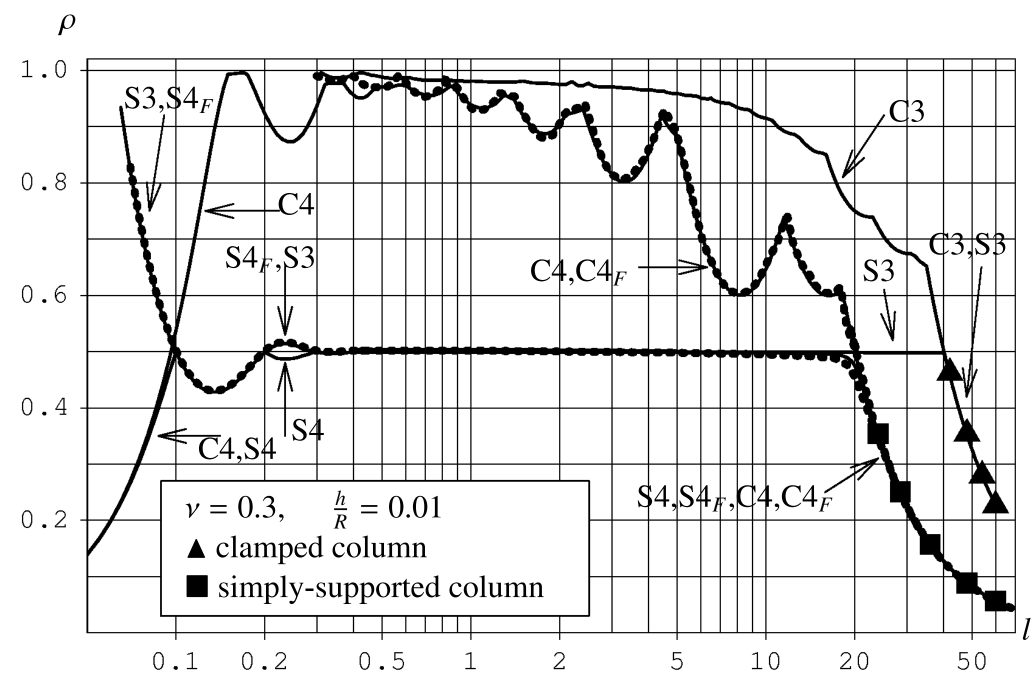

Figure 4: The buckling load of axially compressed perfect cylinder for boundary conditions S3, S4, C3 and C4.

formulations (Fig. 4). With decrease in the cylinder length the corresponding curves by Yamaki (1984) increase and exceed $\rho = 1$, whereas our results show that the resistance to buckling decreases in that range. This discrepancy in asymptotic behaviour of the critical curve for the boundary conditions S4 was revealed already by Simmonds and Danielson (1970), who compared their results with those obtained from the Donnell shell equations, and their result agrees completely with our curve in the S4 case. Simmonds and Danielson (1970) proved this behaviour for short cylinders using the ring–beam theory and cited the similar result noted by Koiter (1967). Similar asymptotic behaviour of the critical load parameter for short cylinders obtained from our stability analysis suggests that it is rather the result of using in our analysis the correct, integrable form of the geometric and associated work–conjugate static boundary conditions.

4.3. Relaxation of geometric boundary conditions as a factor for decreasing the buckling load

The exchange of the geometric boundary constraint $u = 0$ for the static work–conjugate boundary condition $d_1 = 0$ causes the following transition between

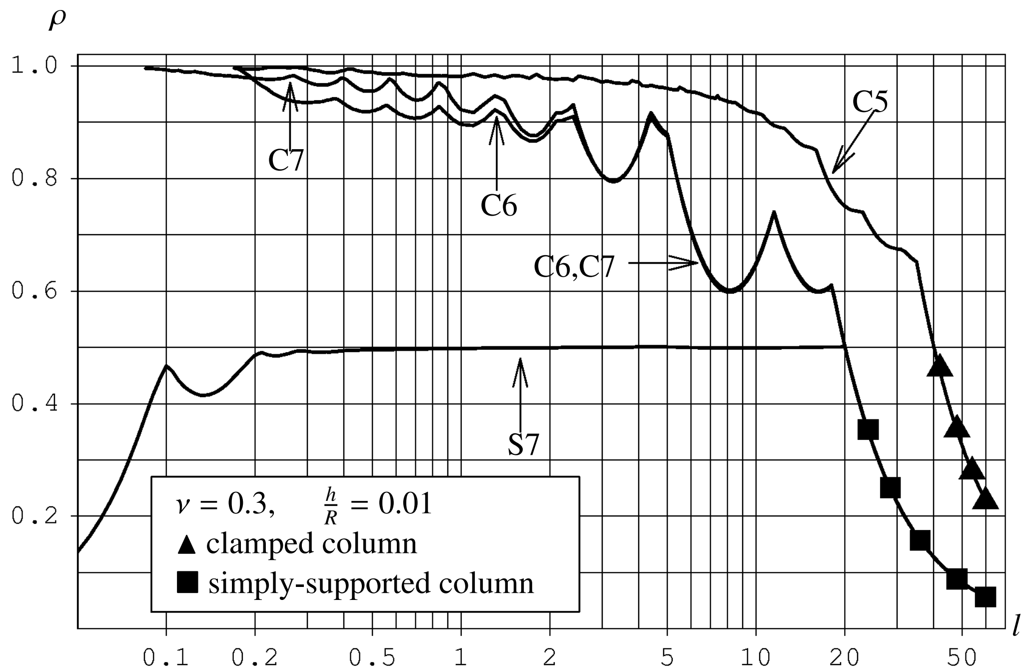

Figure 5: The buckling load of axially compressed perfect cylinder for boundary conditions C5, C6, C7 and S7.

types of boundary conditions: C1→C2, C3→C4, C5→C6, S1→S2, S3→S4 and S5→S6, see Table 1. Generally, this exchange causes that ρ_{crit} takes smaller values and within the range of PCL the difference between the corresponding results increases as the length increases. In the range of ECL the maximal difference is about 20%.

The exchange of boundary constraint $v = 0$ ($w = 0$) for the static work–conjugate boundary condition $d_2 = 0$ ($d_3 = 0$) leading to transitions C1→C3, C2→C4, S5→S7 (C1→C5, C2→C6, S3→S7) causes no effect within PCL. In the transition C5→C7 (C3→C7 for $w = 0$) we have the same behaviour as in the transition C1→C2 described above. Much more interesting are transitions S1→S3 and S2→S4 (S1→S5 and S2→S6 for $w = 0$). In these cases ρ_{crit} falls down to about one half of the classical value in the range of PCL. In cases S1→S3 and S2→S4 this phenomenon was noticed already by Ohira (1961), Hoff and Rehfield (1965), and Almroth (1966). The difference is particularly large for ECL and decreases as the length l increases.

The exchange of the constraint $w' = 0$ for $d_4 = 0$ causes the transition from the clamped to the corresponding simply supported boundary conditions. Essentially the same results are obtained for transitions between practical boundary conditions C1→S1 and C2→S2. But for the remaining ones Ci→Si, i $= 3, .., 7$, ρ_{crit} falls down to about one half of the classical value for PCL. The difference is particularly large for ECL and decreases as the length l increases.

Comparing the results between transitions within the clamped group and within the simply supported group of boundary conditions it is evident, especially for ECL, that the range of changes of ρ_{crit} is much smaller for the clamped group. Therefore, assuring the absence of rotation of the cylinder lateral boundary $w' = 0$ should cause the smaller scatter (due to uncertainty of real boundary conditions) in experimental buckling loads of the axially compressed cylinder. Assuring the condition $w' = 0$ is also important for longer cylinders, within the range of PCL, but differences between the results become smaller.

4.4. Behaviour of long cylinder as Euler column

The buckling load for the axially compressed Euler column with simply-supported (clamped) boundaries is defined in our terms as $\rho = \frac{\pi^2}{16l^2\epsilon}$ ($\rho = \frac{\pi^2}{4l^2\epsilon}$), and its probed values are denoted in Figures 2–5 by black squares (black triangles). It is evident from the results that the axially compressed circular cylinder with the length parameter $l > 20$ and boundary conditions C2, S2, C4, S4, C6, S6, C7 and S7 looses its global stability as the simply-supported Euler column, while the axially compressed very long cylinder $l > 40$ with C1, S1, C3, S3, C5 and S5 boundary conditions behaves itself as the clamped Euler column. Comparing definitions of the boundary conditions given in Table 1, the axially loaded long cylinder behaves as an axially loaded clamped column if its boundaries are constrained as $u = v = 0$ or $u = w = 0$. In the remaining cases the axially loaded long cylinder behaves as an axially loaded simply supported column. Therefore, the condition $u = 0$ indicating that the global rotation of the shell edge as a whole is not allowed, is necessary but not sufficient for the axially loaded long cylinder to behave as an axially loaded clamped column.

For short cylinders, identification of the geometric factors in the boundary conditions C4, S4, S5, S6 and S7 responsible for decrease of ρ_{crit} as l tends to zero takes no effect.

5. Conclusions

This paper has concentrated on two aspects of stability behaviour of the axially compressed circular cylinder: the influence of different boundary conditions and different approximations in the non-linear BVP on the resulting buckling loads. We have noted that:

- The estimation procedure, in which terms of the order of error introduced by the constitutive equations into the BVP have been omitted, leads to elimination of some supposedly small terms from the corresponding shell buckling problem. For long cylinders this elimination results in overestimated buckling loads.

- Using the simplified kinematic relations causes that the buckling load becomes overestimated as well, especially for long cylinders.

- The results obtained from our complete formulation of the shell buckling problem coincide in most cases with the available results following from the Flügge stability equations. However, the entirely different asymptotic behaviour has appeared for S4 and C4 boundary conditions when the length of the short cylinder is decreasing. We explain this behaviour by completeness of work–conjugate boundary conditions used in our analysis.

- Besides the well-known case of relaxing the boundary condition $v = 0$ (transitions S1→S3 and S2→S4), which causes that the buckling load falls down to about one half of the classical value for PCL, we have also discovered that relaxing boundary conditions $w = 0$ (transitions S1→S5 and S2→S6) and $w' = 0$ (transitions Ci→Si, i $= 3, .., 7$) also causes similar effects. Particularly important seem to be the noted dramatic drop of the buckling loads for transitions S1→S3, S2→S4, S1→S5 and S2→S6.

- The wide scatter of numerical results in the range of ECL for simply supported cylinders, contrary the to corresponding small scatter for clamped cylinders, suggests that the buckling load of the axially compressed cylinder is very sensitive to accurate modelling of the rotations allowed at the boundary. Ideally clamped boundary usually assumed in the theoretical and numerical analyses cannot be assured in experiments, because the fixation of the boundary rotation is usually not complete in the test setups. Impossibility to accurately model the real boundary conditions seems to be one of the major reasons of discrepancy between theoretical and experimental buckling loads because according to the most up–to–date experiments presented by Singer et al. (2002) buckling load is in the range $\rho_{crit} \in (0.4, 0.96)$.

References

Almroth, B. O., 1966. Influence of edge conditions on the stability of axially compressed cylindrical shells. AIAA Journal 4 (1), 134–140.

Amabili, M., 2008. Nonlinear Vibrations and Stability of Shells and Plates. Cambridge Univ. Press.

Arbocz, J., Babcock, C. D., 1969. The effect of general imperfections on the buckling of cylindrical shells. Journal of Applied Mechanics 36 (1), 28–38.

Arbocz, J., Starnes, J. H., 2002. Future directions and challenges in shell stability analysis. Thin–Walled Structures 40 (9), 729–754.

Babcock, C. D., 1983. Shell stability. Journal of Applied Mechanics, Trans. ASME 50, 935–940.

Brush, D. O., Almroth, B. O., 1975. Buckling of Bars, Plates, and Shells. New York: McGraw-Hill.

Buchwald, V. T., 1967. Some problems of thin circular cylindrical shells i. the equations. Journal of Mathematics and Physics 46, 237–252.

Buchwald, V. T., 1968. Some problems of thin circular cylindrical shells ii. the infinite crack. Journal of Mathematics and Physics 47, 57–66.

Budiansky, B., 1968. Notes on non-linear shell theory. Journal of Applied Mechanics 35 (2), 393–401.

Bushnell, D., 1981. Buckling of shells–pitfall for designers. AIAA Journal 19 (9), 1183–1226.

Chróścielewski, J., Makowski, J., Pietraszkiewicz, W., 2004. Statics and Dynamisc of Multifold Shells: Nonlinear Theory and the Finie Element Metod (In Polish). Wydawnictwo IPPT PAN, Warszawa.

Donnell, L. H., 1933. Stability of thin-walled tubes under torsion. Report NACA Rep. No. 479.

Dym, C. L., 1973. On the buckling of cylinders in axial compression. Journal of Applied Mechanics 40 (2), 565–568.

Flügge, W., 1932. Die Stabilität der Kreiszylinderschale. Ingenieur Archiv (3), 463–506.

Grigolyuk, E. I., Kabanov, V. V., 1978. Stability of Shells. Moscow: Nauka (In Russian).

Hoff, N. J., Brooklyn, N. Y., 1955. The accuracy of Donnell's equations. Journal of Applied Mechanics 22 (3), 329–334.

Hoff, N. J., Rehfield, L. W., 1965. Buckling of axially compressed circular cylindrical shells at stresses smaller than the classical critical value. Journal of Applied Mechanics 32, 542–546.

Kármán, T., Tsien, H. S., 1941. The buckling of thin cylindrical shells under axial compression. Journal of the Aeronautical Sciences 8 (8), 303–312.

Knight, N. F., Starnes, J. H., 1997. Developments in cylindrical shell stability analysis. AIAA Paper (AIAA-97-1076), 1933–1948.

Koiter, W. T., 1960. A cosistent first approximation in the general theory of shells. In: The Theory of Thin Elastic Shells. Proceedings of the IUTAM Symposium, Delft, 1959. North Holland, Amsterdam, pp. 12–33.

Koiter, W. T., 1967. General equations of elastic stability for thin shells, Appendix: The danger of omitting (supposedly) small buckling terms. In: Proceedings of a Symposium on the Theory of Shells to Honor L. H. Donnell. University of Houston, pp. 225–227.

Lorenz, R., 1911. Die nicht achsensymmetrische Knickung dünnwandiger Hohlzylinder. Physikalische Zeitschrift 12 (7), 241–260.

Mandal, P., Calladine, C. R., 2000. Buckling of thin cylindrical shells under axial compression. International Journal of Solids and Structures 37 (33), 4509–4525.

Mushtari, K. M., Galimov, K. Z., 1957. Nonlinear theory of elastic shells (in Russian). Tatknigoizdat, Kazan', (English transl. : The Israel Program for Sci. Transl. , Monson, Jerusalem 1961).

Ohira, H., 1961. Local buckling theory of axially compressed cylinders. In: Proceedings of the Eleventh Japan National Congress of Applied Mechanics. Tokyo, pp. 37–40.

Opoka, S., Pietraszkiewicz, W., 2009. On modified version of the non-linear theory of thin shells in terms of displacements (submitted to International Journal of Solids and Structures).

Pietraszkiewicz, W., 1977. Introduction to the Nonlinear Theory of Shells. Ruhr-Universität, Inst. für Mech. , Mitt. 10, Bochum.

Pietraszkiewicz, W., 1984. Lagrangian description and incremental formulation in the non-linear theory of thin shells. International Journal of Non-Linear Mechanics 19 (2), 115–140.

Pietraszkiewicz, W., 1993. Explicit Lagrangian incremental and buckling equations for the non-linear theory of thin shells. International Journal of Non-Linear Mechanics 28 (2), 209–220.

Pietraszkiewicz, W., Szwabowicz, M. L., 1981. Entirely Lagrangian nonlinear theory of thin shells. Archives of Mechanics 33 (2), 273–288.

Pircher, M., Berry, P. A., Ding, X., Bridge, R. Q., 2001. The shape of circumferential weld-induced imperfections in thin-walled steel silos and tanks. Thin-Walled Structures 39 (12), 999–1014.

Riks, E., 1998. Buckling analyses of elastic structures: A computational approach. Advances of Applied Mechanics 34, 1–76.

Sanders, J. L., 1963. Nonlinear theories for thin shells. Quarterly of Applied Mathematics 21 (1), 21–36.

Simitses, G. J., 1986. Buckling and postbuckling of imperfect cylindrical shells: A review. Applied Mechanics Reviews 39 (10), 1517–1524.

Simmonds, J. G., Danielson, D. A., 1970. New results for the buckling loads of axially compressed cylindrical shells subject to relaxed boundary conditions. Journal of Applied Mechanics 37 (1), 93–100.

Singer, J., Arbocz, J., Weller, T., 2002. Buckling Experiments: Experimental Methods in Buckling of Thin-Walled Structures. Vol. 2. New-York: Wiley.

Sobel, L. H., 1964. Effects of boundary conditions on the stability of cylinders subject to lateral and axial pressures. AIAA Journal 2 (8), 1437–1440.

Stumpf, H., 1984. On the nonlinear buckling and postbuckling analysis of thin elastic shells. International Journal of Non–Linear Mechanics 19 (3), 195–215.

Tovstik, P., Smirnov, A. L., 2001. Asymptotic Methods in the Buckling Theory of Elastic Shells. World Scientific, Singapore.

Vol'mir, A. S., 1967. Stability of Deformable Systems, 2nd ed. Nauka, Moscow (In Russian).

Weingarten, V. I., Morgan, E. J., Seide, P., 1965. Elastic stability of thin-walled cylindrical and conical shells under axial compression. AIAA Journal 3 (3), 500–505.

Wriggers, P., 2008. Nonlinear Finite Element Methods. Springer, Berlin.

Yamaki, N., 1984. Elastic Stability of Circular Cylindrical Shells. Elsevier, Amsterdam.

A. Appendix: Boundary value and buckling problems for thin circular cylinder

A.1. Geometry of the finite perfect cylinder

The position vector of the circular cylindrical surface $\mathscr{M}$ is postulated in the form, see Fig. 6,

$$\mathbf{r} = R\cos\phi\,\mathbf{i} + R\sin\phi\,\mathbf{j} + z\,\mathbf{k}\ , \tag{A-1}$$

where R is the radius of the cylinder. The surface curvilinear coordinates vary in the ranges $\phi \in (0, 2\pi]$ and $z \in [-L/2, L/2]$, where L is the length of the cylinder. The frame $\{\mathbf{i}, \mathbf{j}, \mathbf{k}\}$ denotes the orthonormal base in the Euclidean space. Taking into account (A-1) and assuming that $(\theta^1, \theta^2) = (\phi, z)$, the surface base vectors in $\mathscr{M}$ are

$$\begin{aligned}
\mathbf{a}_1 &= \frac{\partial\mathbf{r}}{\partial\phi} = -R\sin\phi\,\mathbf{i} + R\cos\phi\,\mathbf{j}\ , &\qquad \mathbf{a}_2 &= \frac{\partial\mathbf{r}}{\partial z} = \mathbf{k}\ ,\\
\mathbf{a}^1 &= \frac{\mathbf{a}_2\times\mathbf{n}}{\mathbf{a}_1\cdot(\mathbf{a}_2\times\mathbf{n})} = -\frac{1}{R}(\sin\phi\,\mathbf{i} - \cos\phi\,\mathbf{j})\ , &\qquad \mathbf{a}^2 &= \frac{\mathbf{n}\times\mathbf{a}_1}{\mathbf{a}_1\cdot(\mathbf{a}_2\times\mathbf{n})} = \mathbf{k}\ ,\\
\mathbf{n} &= \frac{\mathbf{a}_1\times\mathbf{a}_2}{|\mathbf{a}_1\times\mathbf{a}_2|} = \cos\phi\,\mathbf{i} + \sin\phi\,\mathbf{j}\ .
\end{aligned} \tag{A-2}$$

Using (A-2) we can calculate the contravariant components $a^{\alpha\beta}$ of the metric tensor, mixed components b^{α}_{β} of the curvature tensor, and Christoffel symbols $\Gamma^{\lambda}_{\alpha\beta}$ of the cylinder:

$$a^{\alpha\beta} = \begin{bmatrix} R^{-2} & 0 \\ 0 & 1 \end{bmatrix}, \quad b^{\alpha}_{\beta} = \begin{bmatrix} -R^{-1} & 0 \\ 0 & 0 \end{bmatrix}, \quad \Gamma^{1}_{\alpha\beta} = \Gamma^{2}_{\alpha\beta} = \begin{bmatrix} 0 & 0 \\ 0 & 0 \end{bmatrix}. \tag{A-3}$$

Since all Christoffel symbols vanish, the covariant differentiation on the cylinder reduces to the partial differentiation.

We assume that both boundaries $\partial\mathscr{M}_1$ and $\partial\mathscr{M}_2$ of the cylinder are perpendicular to its generators. With every point of $\partial\mathscr{M}$ we associate the orthonormal triad $\{\boldsymbol{\tau}, \boldsymbol{\nu}, \mathbf{n}\}$. Since the vector $\mathbf{n}$ is already defined in (A-2) and the unit normal $\boldsymbol{\nu}$ is always assumed to be directed outward of $\partial\mathscr{M}$, the direction of $\boldsymbol{\tau}$ is uniquely established by the right-handed cross product, see Fig. 6. Comparing

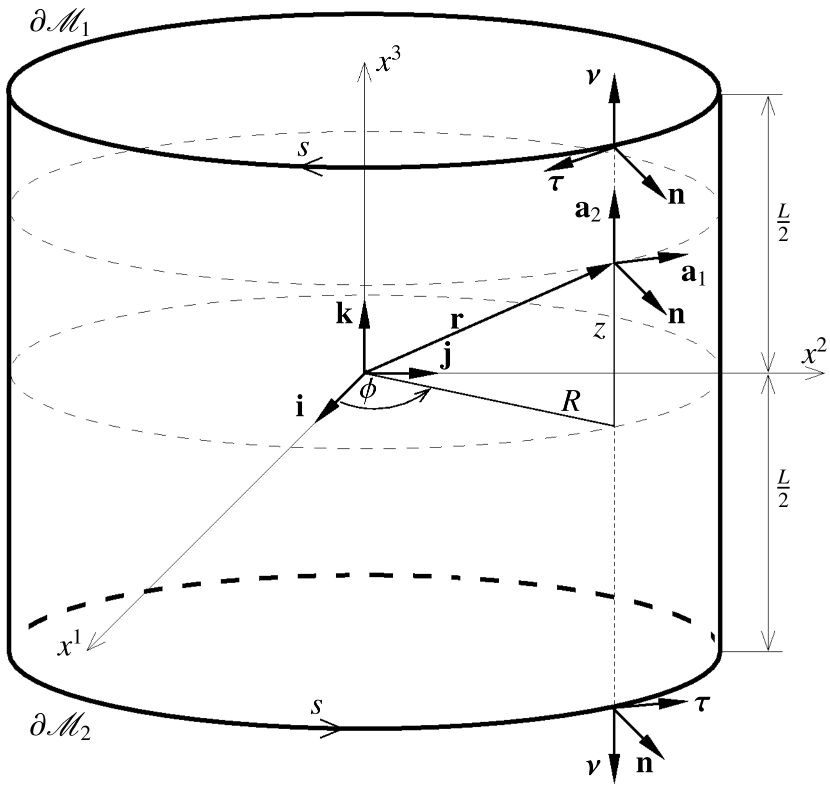

Figure 6: Surface and boundary base vectors on the cylinder.

directions between the boundary and surface base vectors and using the relations

$\tau^{\alpha}\tau_{\alpha} = \nu^{\alpha}\nu_{\alpha} = 1$, the components of boundary vectors $\boldsymbol{\tau}$ and $\boldsymbol{\nu}$ read (upper signs correspond to $\partial\mathscr{M}_1$, lower ones to $\partial\mathscr{M}_2$)

$$\tau_1 = \mp R\ , \quad \tau^1 = \mp R^{-1}\ , \quad \nu_2 = \nu^2 = \pm 1\ , \quad \tau^2 = \tau_2 = \nu^1 = \nu_1 = 0\ . \qquad \text{(A-4)}$$

Using (A-3) and (A-4), the curvatures and torsions of $\partial\mathscr{M}_1$ and $\partial\mathscr{M}_2$ are

$$\sigma_\tau = -R^{-1}\ , \quad \sigma_\nu = \tau_\tau = \tau_\nu = \rho_\tau = \rho_\nu = 0\ . \qquad \text{(A-5)}$$

The quantities presented here were obtained using the package *ShellGeom.m*.

A.2. Non-dimensional variables

All quantities appearing in the non-linear BVP of thin elastic shells formulated by Opoka and Pietraszkiewicz (2009) are supposed to be defined in appropriate SI units. Denoting by $[\cdot]$ SI units of the quantity, various fields of our problem have units indicated below

$$\begin{aligned}
&[\phi, \nu, \epsilon, A_{\langle 2\rangle}, \boldsymbol{\nu}, \boldsymbol{\tau}, \mathbf{n}, \mathbf{a}_2, \mathbf{a}^2, \mathbf{e}_{\langle 1\rangle}, \mathbf{e}_{\langle 2\rangle}, \mathbf{a} = \delta^{\alpha}_{\beta}\mathbf{a}_{\alpha}\otimes\mathbf{a}^{\beta}, \boldsymbol{\gamma} = \gamma_{\alpha\beta}\mathbf{a}^{\alpha}\otimes\mathbf{a}^{\beta}] = 1\ ,\\
&[A] = \frac{m}{N}\ , \quad [D] = N\cdot m\ , \quad [\mathbf{N} = N^{\alpha\beta}\bar{\mathbf{a}}_{\alpha}\otimes\bar{\mathbf{a}}_{\beta}, \mathbf{N}^{*} = N^{*}_{\nu}\boldsymbol{\nu} + N^{*}_{\tau}\boldsymbol{\tau} + N^{*}\mathbf{n}, \mathbf{h} = m^{\alpha}\bar{\mathbf{a}}_{\alpha}] = \frac{N}{m}\ ,\\
&[\mathbf{b} = b^{\alpha}_{\beta}\mathbf{a}_{\alpha}\otimes\mathbf{a}^{\beta}, \boldsymbol{\chi} = \chi_{\alpha\beta}\mathbf{a}^{\alpha}\otimes\mathbf{a}^{\beta}, \mathbf{a}^1] = \frac{1}{m}\ , \quad [E, \mathbf{p} = p_{\alpha}\bar{\mathbf{a}}^{\alpha} + p\bar{\mathbf{n}}] = \frac{N}{m^2}\ ,\\
&[\mathbf{M} = M^{\alpha\beta}\bar{\mathbf{a}}_{\alpha}\otimes\bar{\mathbf{a}}_{\beta}, \mathbf{H}^{*} = M^{*}_{\nu}\bar{\boldsymbol{\nu}} + M^{*}_{\tau}\bar{\boldsymbol{\tau}}] = N\ , \quad [z, h, R, A_{\langle 1\rangle}, \mathbf{a}_1, \mathbf{u}] = m\ .
\end{aligned} \qquad \text{(A-6)}$$

The independent variable ϕ is already non-dimensional. For the coordinate z we postulate change of variables $z = R\,x$, where the new non-dimensional variable x is introduced. This change affects partial differentiation on the cylinder $\frac{\partial}{\partial z^n} = \frac{1}{R^n}\frac{\partial}{\partial x^n}$. Since $d\mathbf{s} = \mathbf{a}_1 d\phi$, $ds^2 = R^2\,(d\phi)^2$ and $d\mathbf{s}_\nu = \mathbf{a}_2 dz$, $ds_\nu^2 = (dz)^2 = R^2\,(dx)^2$, it also affects partial differentiation at the cylinder boundaries:

$$(\cdot),_s = (\cdot),_\alpha\,\tau^{\alpha} = \mp\tfrac{1}{R}\tfrac{\partial}{\partial\phi}(\cdot)\ , \quad (\cdot),_\nu = (\cdot),_\alpha\,\nu^{\alpha} = \pm\tfrac{1}{R}\tfrac{\partial}{\partial x}(\cdot)\ . \qquad \text{(A-7)}$$

In order to express any second order tensor in terms of components having the same physical meaning, we must rewrite the tensor in a non-dimensional unit base vectors. In orthogonal coordinates we have $a_{12} = 0$ and any second order tensor $\mathbf{T}$ can be expressed as

$$\mathbf{T} = T^{\alpha}_{\beta}\mathbf{a}_{\alpha}\otimes\mathbf{a}^{\beta} = \Big(T^{\alpha}_{\beta}\frac{A_{\langle\alpha\rangle}}{A_{\langle\beta\rangle}}\Big)\mathbf{e}_{\langle\alpha\rangle}\otimes\mathbf{e}_{\langle\beta\rangle}\ , \qquad \text{(A-8)}$$

where the non-dimensional unit base vectors are denoted by $\mathbf{e}_{\langle\alpha\rangle}$, and $A_{\langle\alpha\rangle} = \sqrt{\mathbf{a}_\alpha \cdot \mathbf{a}_\alpha}$. The terms in parentheses in (A-8), called the physical components of the tensor $\mathbf{T}$, are expressed in the same physical units as the corresponding surface tensor $\mathbf{T}$ itself. From (A-6) we note that the surface strain tensor $\boldsymbol{\gamma}$, the modified surface curvature tensor $\boldsymbol{\chi}$ (where $\chi_{\alpha\beta} = \sqrt{\frac{\bar{a}}{a}}\bar{b}_{\alpha\beta}$) and the surface displacement vector $\mathbf{u}$ have the same physical dimensions as 1, $1/R^2$ and R, respectively.

Using (A-4) and (A-8), and taking into account that now $A_{\langle 1\rangle} = R$, $A_{\langle 2\rangle} = 1$, mixed components γ^α_β and χ^α_β, contravariant components of $\mathbf{u}$ as well as their physical components at the boundary, components of the surface load $\mathbf{p}$ and the surface moment $\mathbf{h}$, as well as components of the boundary force $\mathbf{N}^*$ and the boundary moment $\mathbf{H}^*$ can be expressed in terms of the following non-dimensional functions:

$$
\begin{aligned}
&\gamma^1_1 = \gamma_{\tau\tau} = \gamma_\phi(\phi, x)\ , && \gamma^2_2 = \gamma_{\nu\nu} = \gamma_x(\phi, x)\ , && \gamma^2_1 = R^2\gamma^1_2 = -R\gamma_{\nu\tau} = R\gamma_{x\phi}(\phi, x)\ ,\\
&\chi^1_1 = \chi_{\tau\tau} = \tfrac{1}{R}\chi_\phi(\phi, x)\ , && \chi^2_2 = \chi_{\nu\nu} = \tfrac{1}{R}\chi_x(\phi, x)\ , && \chi^2_1 = R^2\chi^1_2 = -R\chi_{\nu\tau} = \chi_{x\phi}(\phi, x)\ ,\\
&u^1 = \mp\tfrac{1}{R}u_\tau = v(\phi, x)\ , && u^2 = \pm u_\nu = R\, u(\phi, x)\ , && u^3 = u_3 = R\, w(\phi, x)\ ,\\
&p_1 = \tfrac{D}{R^2}p_\phi(\phi, x)\ , && p_2 = \tfrac{D}{R^3}p_x(\phi, x)\ , && p = \tfrac{D}{R^3}p(\phi, x)\ ,\\
&c^1 = \tfrac{1}{R^2}c_1 = \tfrac{D}{R^3}c_\phi(\phi, x)\ , && c^2 = c_2 = \tfrac{D}{R^2}c_x(\phi, x)\ , && \\
&N^*_\nu = \tfrac{D}{R^2}N^*_\nu(\phi, x)\ , && N^*_\tau = \tfrac{D}{R^2}N^*_\tau(\phi, x)\ , && N^* = \tfrac{D}{R^2}N^*(\phi, x)\ ,\\
&M^*_\nu = \tfrac{D}{R}M^*_\nu(\phi, x)\ , && M^*_\tau = \tfrac{D}{R}M^*_\tau(\phi, x)\ . &&
\end{aligned}
\tag{A-9}
$$

Please note that some of the relations in (A-4), (A-7), and (A-9) have different signs at two different boundaries of the cylinder. Therefore, when only half of the cylinder is analysed the forms of boundary condition at different boundaries must be checked whether they are the same indeed.

A.3. The equilibrium BVP for the finite cylinder

Let us transform the BVP (Opoka and Pietraszkiewicz, 2009, eqs. (21), (41)) in the following way:

- substitute the constitutive equations of the first–approximation geometrically non–linear theory of thin elastic shells for $N^{\alpha\beta}$, $M^{\alpha\beta}$ and introduce χ^α_β (Opoka and Pietraszkiewicz, 2009, eqs. (44), $(3)_2$), then apply the relations $\left(\sqrt{\frac{a}{\bar{a}}}\right)|_\beta = -\left(\frac{a}{\bar{a}}\right)^{\frac{3}{2}} g_\beta$, $\left(\sqrt{\frac{a}{\bar{a}}}\right)|_{\beta\alpha} = 3\left(\frac{a}{\bar{a}}\right)^{\frac{5}{2}} g_\beta g_\alpha - \left(\frac{a}{\bar{a}}\right)^{\frac{3}{2}} g_\beta|_\alpha$, $\left(\frac{a}{\bar{a}}\right)|_\beta = -2\left(\frac{a}{\bar{a}}\right)^2 g_\beta$, where $g_\beta = (1 + 2\gamma^\lambda_\lambda)\gamma^\alpha_\alpha|_\beta - 2\gamma^\lambda_\alpha\gamma^\alpha_\lambda|_\beta$;

- multiply two tangential equilibrium equations by $(\frac{\bar{a}}{a})^2$, the third one by $(\frac{\bar{a}}{a})^{\frac{5}{2}}$, while the first three static boundary conditions by $\frac{\bar{a}}{a} l^2_{\tau\tau}$ and the fourth one by $(\frac{\bar{a}}{a})^{\frac{1}{2}}$, and then expand covariant derivatives and expressions containing dummy indices;
- substitute geometric quantities (A-3), (A-4) and (A-5), change the independent variable $z = Rx$, use (A-7) and introduce non-dimensional functions (A-9).

Then the equilibrium equations (Opoka and Pietraszkiewicz, 2009, eq. (21)) are transformed to the following system of three PDEs in strains $\gamma_{x\phi}$, γ_x, γ_ϕ and modified curvatures $\chi_{x\phi}$, χ_x, χ_ϕ as intermediate dependent variables that describe the deformed state of the cylinder:

$$
\begin{aligned}
&(\tfrac{\bar{a}}{a})^2\Big\{(1-\nu+2\gamma_\phi+2\gamma_x)\gamma'_{x\phi}+(1+3\gamma_\phi+\nu\gamma_x)\gamma^{\bullet}_{\phi}+(\nu+\nu\gamma_\phi-\gamma_x)\gamma^{\bullet}_{x}+2\gamma_{x\phi}[\gamma'_\phi+\gamma'_x+(1-\nu)\gamma^{\bullet}_{x\phi}]\Big\}\\
&+\epsilon^2(1-\nu^2)\Big\{\tfrac{\bar{a}}{a}[\chi_\phi(2\chi'_{x\phi}+3\chi^{\bullet}_{\phi}+\nu\chi^{\bullet}_{x})+2\chi_{x\phi}(\chi'_\phi+\chi'_x+(1-\nu)\chi^{\bullet}_{x\phi})+\chi_x(2\chi'_{x\phi}+\nu\chi^{\bullet}_{\phi}-\chi^{\bullet}_{x})]\\
&-\Big[3\chi^2_\phi+2\nu\chi_\phi\chi_x-\chi^2_x+2(1-\nu)\chi^2_{x\phi}+\sqrt{\tfrac{\bar{a}}{a}}(\chi_\phi-\nu\chi_x)\Big][(1+2\gamma_x)\gamma^{\bullet}_{\phi}+(1+2\gamma_\phi)\gamma^{\bullet}_{x}-4\gamma_{x\phi}\gamma^{\bullet}_{x\phi}]\\
&-2\chi_{x\phi}\Big[2(\chi_\phi+\chi_x)+\sqrt{\tfrac{\bar{a}}{a}}\nu\Big][(1+2\gamma_x)\gamma'_\phi+(1+2\gamma_\phi)\gamma'_x-4\gamma_{x\phi}\gamma'_{x\phi}]+(\tfrac{\bar{a}}{a})^{\frac{3}{2}}(\chi^{\bullet}_{\phi}+2\nu\chi'_{x\phi}-\nu\chi^{\bullet}_{x}\\
&-\chi_\phi c_\phi-\chi_{x\phi}c_x)+(\tfrac{\bar{a}}{a})^2 p_\phi\Big\}=0\ ,
\end{aligned}
$$

$$
\begin{aligned}
&(\tfrac{\bar{a}}{a})^2\Big\{(1-\nu+2\gamma_\phi+2\gamma_x)\gamma^{\bullet}_{x\phi}+(\nu+\nu\gamma_x-\gamma_\phi)\gamma'_\phi+(1+\nu\gamma_\phi+3\gamma_x)\gamma'_x+2\gamma_{x\phi}[\gamma^{\bullet}_{\phi}+\gamma^{\bullet}_{x}+(1-\nu)\gamma'_{x\phi}]\Big\}\\
&+\epsilon^2(1-\nu^2)\Big\{\tfrac{\bar{a}}{a}[\chi_\phi(2\chi^{\bullet}_{x\phi}-\chi'_\phi+\nu\chi'_x)+2\chi_{x\phi}(\chi^{\bullet}_{x}+(1-\nu)\chi'_{x\phi}+\chi^{\bullet}_{\phi})+\chi_x(2\chi^{\bullet}_{x\phi}+\nu\chi'_\phi+3\chi'_x)]\\
&-\Big[3\chi^2_x+2\nu\chi_\phi\chi_x-\chi^2_\phi+2(1-\nu)\chi^2_{x\phi}-\sqrt{\tfrac{\bar{a}}{a}}(\chi_\phi-\nu\chi_x)\Big][(1+2\gamma_x)\gamma'_\phi+(1+2\gamma_\phi)\gamma'_x-4\gamma_{x\phi}\gamma'_{x\phi}]\\
&-2\chi_{x\phi}\Big[2(\chi_\phi+\chi_x)+\sqrt{\tfrac{\bar{a}}{a}}\Big][(1+2\gamma_x)\gamma^{\bullet}_{\phi}+(1+2\gamma_\phi)\gamma^{\bullet}_{x}-4\gamma_{x\phi}\gamma^{\bullet}_{x\phi}]-(\tfrac{\bar{a}}{a})^{\frac{3}{2}}(\chi'_\phi-\nu\chi'_x-2\chi^{\bullet}_{x\phi}\\
&+\chi_{x\phi}c_\phi+\chi_x c_x)+(\tfrac{\bar{a}}{a})^2 p_x\Big\}=0\ ,
\end{aligned}
$$

$$
\begin{aligned}
&(\tfrac{\bar{a}}{a})^2\Big\{(\chi_\phi+\nu\chi_x)\gamma_\phi+(\chi_x+\nu\chi_\phi)\gamma_x+2(1-\nu)\chi_{x\phi}\gamma_{x\phi}-\epsilon^2(1-\nu^2)\Big[\chi''_x+\chi^{\bullet\bullet}_{\phi}+2(1-\nu)\chi'^{\bullet}_{x\phi}\\
&+\nu(\chi''_\phi+\chi^{\bullet\bullet}_{x})-\sqrt{\tfrac{\bar{a}}{a}}(p+c'_x+c^{\bullet}_{\phi})\Big]\Big\}-\epsilon^2(1-\nu^2)\Big(d_0-\sqrt{\tfrac{\bar{a}}{a}}d_1-\tfrac{\bar{a}}{a}d_2-(\tfrac{\bar{a}}{a})^{\frac{3}{2}}d_3\Big)=0\ ,
\end{aligned}
\tag{A-10}
$$

where the expressions d_i in $(\text{A-10})_3$ are

$$
\begin{aligned}
d_0 =\;& 6(1-\nu)\chi_{x\phi}\Big\{(1+2\gamma_x)[(1+2\gamma_\phi)(\gamma'_x\gamma^{\bullet}_\phi-\gamma'_\phi\gamma^{\bullet}_x)+2\gamma_{x\phi}({\gamma'_\phi}^2+\gamma^{\bullet}_\phi(\gamma^{\bullet}_x-2\gamma'_{x\phi}))]+2(1+2\gamma_\phi)\gamma_{x\phi}[{\gamma^{\bullet}_x}^2\\
&+\gamma'_x(\gamma'_\phi-2\gamma^{\bullet}_{x\phi})]-8\gamma^2_{x\phi}[\gamma'_\phi\gamma'_{x\phi}+\gamma^{\bullet}_{x\phi}(\gamma^{\bullet}_x-2\gamma'_{x\phi})]\Big\}-(1+2\gamma_\phi)[(\chi_\phi+(2-\nu)\chi_x)\chi^2_{x\phi}+(\chi_x+\nu\chi_\phi)\chi^2_x]\\
&+4\gamma_{x\phi}\chi_{x\phi}[\chi^2_\phi+\chi^2_x+(1+\nu)\chi_\phi\chi_x+(1-\nu)\chi^2_{x\phi}]-(1+2\gamma_x)[(\chi_x+(2-\nu)\chi_\phi)\chi^2_{x\phi}+(\chi_\phi+\nu\chi_x)\chi^2_\phi]\\
&+3(\chi_\phi+\nu\chi_x)\Big\{8\gamma^2_{x\phi}(\gamma^{\bullet}_{x\phi}\gamma'_\phi-\gamma'_{x\phi}\gamma^{\bullet}_\phi)+(1+2\gamma_x)(1+2\gamma_\phi)[\gamma^{\bullet}_\phi\gamma^{\bullet}_x+\gamma'_\phi(\gamma'_\phi-2\gamma^{\bullet}_{x\phi})]\\
&+(1+2\gamma_\phi)^2[{\gamma^{\bullet}_x}^2+\gamma'_x(\gamma'_\phi-2\gamma^{\bullet}_{x\phi})]+2(1+2\gamma_\phi)\gamma_{x\phi}[\gamma'_x\gamma^{\bullet}_\phi+2(2\gamma'_{x\phi}-\gamma^{\bullet}_x)\gamma^{\bullet}_{x\phi}-\gamma'_\phi(2\gamma'_{x\phi}+\gamma^{\bullet}_x)]\Big\}\\
&+3(\chi_x+\nu\chi_\phi)\Big\{8\gamma^2_{x\phi}(\gamma'_{x\phi}\gamma^{\bullet}_x-\gamma^{\bullet}_{x\phi}\gamma'_x)+(1+2\gamma_x)(1+2\gamma_\phi)[\gamma'_\phi\gamma'_x+\gamma^{\bullet}_x(\gamma^{\bullet}_x-2\gamma'_{x\phi})]\\
&+(1+2\gamma_x)^2[{\gamma'_\phi}^2+\gamma^{\bullet}_\phi(\gamma^{\bullet}_x-2\gamma'_{x\phi})]+2(1+2\gamma_x)\gamma_{x\phi}[\gamma'_x\gamma^{\bullet}_\phi+2(2\gamma'_{x\phi}-\gamma^{\bullet}_x)\gamma^{\bullet}_{x\phi}-\gamma'_\phi(2\gamma'_{x\phi}+\gamma^{\bullet}_x)]\Big\}\;,
\end{aligned}
$$

$$
\begin{aligned}
d_1 =\;& 2\{8\gamma^2_{x\phi}\gamma'_{x\phi}+(1+2\gamma_x)[(1+2\gamma_x)\gamma^{\bullet}_\phi+(1+2\gamma_\phi)\gamma^{\bullet}_x-2\gamma_{x\phi}(\gamma'_\phi+2\gamma^{\bullet}_{x\phi})]-2\gamma_{x\phi}(1+2\gamma_\phi)\gamma'_x\}\\
&(\gamma^{\bullet}_\phi-\nu\gamma^{\bullet}_x+2\nu\gamma'_{x\phi})-2\{8\gamma^2_{x\phi}\gamma^{\bullet}_{x\phi}+(1+2\gamma_\phi)[(1+2\gamma_x)\gamma'_\phi+(1+2\gamma_\phi)\gamma'_x-2\gamma_{x\phi}(\gamma^{\bullet}_x+2\gamma'_{x\phi})]\\
&-2\gamma_{x\phi}(1+2\gamma_x)\gamma^{\bullet}_\phi\}(\gamma'_\phi-\nu\gamma'_x-2\gamma^{\bullet}_{x\phi})+(1+2\gamma_\phi)(\chi^2_{x\phi}+\nu\chi^2_x)+(1+2\gamma_x)(\chi^2_\phi+\nu\chi^2_{x\phi})-4\gamma_{x\phi}\chi_{x\phi}(\chi_\phi+\nu\chi_x)\;,
\end{aligned}
$$

$$
\begin{aligned}
d_2 =\;& 2(1-\nu)\{\chi'_{x\phi}[2\gamma_{x\phi}\gamma'_\phi-(1+2\gamma_\phi)\gamma^{\bullet}_x]-\chi^{\bullet}_{x\phi}[(1+2\gamma_x)\gamma'_\phi-2\gamma_{x\phi}\gamma^{\bullet}_x]\}-2(1+\nu)(\chi_\phi+\chi_x)\gamma'^{\bullet}_{x\phi}\\
&+(\chi'_\phi+\nu\chi'_x)[(1+2\gamma_\phi)(\gamma'_\phi-2\gamma^{\bullet}_{x\phi})+2\gamma_{x\phi}\gamma^{\bullet}_\phi]-(\chi^{\bullet}_\phi+\nu\chi^{\bullet}_x)[(1+2\gamma_x)\gamma^{\bullet}_\phi+2\gamma_{x\phi}(\gamma'_\phi-2\gamma^{\bullet}_{x\phi})]\\
&+(\chi^{\bullet}_x+\nu\chi^{\bullet}_\phi)[(1+2\gamma_x)(\gamma^{\bullet}_x-2\gamma'_{x\phi})+2\gamma_{x\phi}\gamma'_x]-(\chi'_x+\nu\chi'_\phi)[(1+2\gamma_\phi)\gamma'_x+2\gamma_{x\phi}(\gamma^{\bullet}_x-2\gamma'_{x\phi})]\\
&+4(1-\nu)\chi_{x\phi}[\gamma_{x\phi}(\gamma''_\phi-2\gamma'^{\bullet}_{x\phi}+\gamma^{\bullet\bullet}_x)+\gamma'_x\gamma^{\bullet}_\phi+\gamma'_\phi(\gamma'_{x\phi}-\gamma^{\bullet}_x)-\gamma^{\bullet}_{x\phi}(2\gamma'_{x\phi}-\gamma^{\bullet}_x)]\\
&+(\chi_x+\nu\chi_\phi)[(1+2\gamma_x)(\gamma''_\phi+\gamma^{\bullet\bullet}_x)-4\gamma_x\gamma'^{\bullet}_{x\phi}+2\gamma^{\bullet}_x(\gamma^{\bullet}_x-3\gamma'_{x\phi})+2\gamma'_x(\gamma'_\phi+\gamma^{\bullet}_{x\phi})]\\
&+(\chi_\phi+\nu\chi_x)[(1+2\gamma_\phi)(\gamma''_\phi+\gamma^{\bullet\bullet}_x)-4\gamma_\phi\gamma'^{\bullet}_{x\phi}+2\gamma'_\phi(\gamma'_\phi-3\gamma^{\bullet}_{x\phi})+2\gamma^{\bullet}_\phi(\gamma^{\bullet}_x+\gamma'_{x\phi})]\;,
\end{aligned}
$$

$$
\begin{aligned}
d_3 =\;& 2[\gamma'_\phi(\gamma'_\phi-\nu\gamma'_x-3\gamma^{\bullet}_{x\phi})+\gamma'_{x\phi}(\gamma^{\bullet}_\phi+2\nu\gamma'_{x\phi}-3\nu\gamma^{\bullet}_x)+\gamma^{\bullet}_{x\phi}(2\gamma^{\bullet}_{x\phi}+\nu\gamma'_x)-\gamma^{\bullet}_x(\gamma^{\bullet}_\phi-\nu\gamma^{\bullet}_x)]\\
&-(1+2\gamma_x)(\gamma^{\bullet\bullet}_\phi-\nu\gamma^{\bullet\bullet}_x+2\nu\gamma'^{\bullet}_{x\phi})+(1+2\gamma_\phi)(\gamma''_\phi-\nu\gamma''_x-2\gamma'^{\bullet}_{x\phi})+4\gamma_{x\phi}(\gamma^{\bullet\bullet}_{x\phi}+\nu\gamma''_{x\phi})\;.
\end{aligned}
\tag{A-11}
$$

The small parameter ϵ in (A-10) is defined as $\epsilon^2 = AD/R^2 = h^2/[12(1-\nu^2)R^2]$, and partial derivatives are denoted as $()_{,x} = ()'$, $()_{,\phi} = ()^{\bullet}$.

The work–conjugate boundary conditions (Opoka and Pietraszkiewicz, 2009, eq. (41)) at $x = \pm l$, $l = L/2R$, are transformed to the following form expressed in surface strains $\gamma_{x\phi}$, γ_x, γ_ϕ, modified curvatures $\chi_{x\phi}$, χ_x, χ_ϕ and displacements u, v,

w:

$$
\begin{aligned}
&l_{\nu\nu}(\mathcal{C}_\nu-\mathcal{G}_\nu^*)+l_{\nu\tau}(\mathcal{C}_\tau-\mathcal{G}_\tau^*)+m_\nu(\mathcal{D}-\mathcal{F}^*,_s)-\mathcal{K}N_\nu^*=0 \quad &&\text{or} \quad u=\pm\tfrac{1}{R}C_1\ ,\\
&l_{\tau\nu}(\mathcal{C}_\nu-\mathcal{G}_\nu^*)+l_{\tau\tau}(\mathcal{C}_\tau-\mathcal{G}_\tau^*)+m_\tau(\mathcal{D}-\mathcal{F}^*,_s)-\mathcal{K}N_\tau^*=0 \quad &&\text{or} \quad v=\mp\tfrac{1}{R}C_2\ ,\\
&\varphi_\nu(\mathcal{C}_\nu-\mathcal{G}_\nu^*)+\varphi_\tau(\mathcal{C}_\tau-\mathcal{G}_\tau^*)+m(\mathcal{D}-\mathcal{F}^*,_s)-\mathcal{K}N^*=0 \quad &&\text{or} \quad w=\tfrac{1}{R}C_3\ ,\\
&\chi_x+\nu\chi_\phi+\sqrt{\tfrac{\bar a}{a}}\nu+a_\tau M_\nu^*=0 \quad &&\text{or} \quad m_\nu=C_4 m\ .
\end{aligned}
\tag{A-12}
$$

The coefficients appearing in (A-12) are defined by

$$
\begin{aligned}
&l_{\nu\nu}=1+u'\ , && l_{\nu\tau}=-u^{\boldsymbol{\cdot}}\ , && m_\nu=\pm[v'(w^{\boldsymbol{\cdot}}-v)-w'(1+w+v^{\boldsymbol{\cdot}})]\ ,\\
&l_{\tau\tau}=1+w+v^{\boldsymbol{\cdot}}\ , && l_{\tau\nu}=-v'\ , && m_\tau=\pm[(w^{\boldsymbol{\cdot}}-v)(1+u')-w'u^{\boldsymbol{\cdot}}]\ ,\\
&\varphi_\nu=\pm w'\ , && \varphi_\tau=\pm(v-w^{\boldsymbol{\cdot}})\ , && m=(1+w+v^{\boldsymbol{\cdot}})(1+u')-v'u^{\boldsymbol{\cdot}}\ ,
\end{aligned}
\tag{A-13}
$$

and

$$
\begin{aligned}
\mathcal{C}_\nu =&(\tfrac{\bar a}{a})^2(1+w+v^{\boldsymbol{\cdot}})^2(\gamma_x+\nu\gamma_\phi)+\epsilon^2(1-\nu^2)\Big\{(1+w+v^{\boldsymbol{\cdot}})^2\Big(\chi_x+\nu\chi_\phi+\sqrt{\tfrac{\bar a}{a}}\nu\Big)[(1+2\gamma_\phi)\chi_x-2\gamma_{x\phi}\chi_{x\phi}]\\
&+\Big[2(1-\nu)(1+w+v^{\boldsymbol{\cdot}})^2\chi_{x\phi}+v'(1+w+v^{\boldsymbol{\cdot}})\Big(\chi_x+\nu\chi_\phi+\sqrt{\tfrac{\bar a}{a}}\nu\Big)\Big][(1+2\gamma_\phi)\chi_{x\phi}-2\gamma_{x\phi}\chi_\phi]\Big\}\ ,\\
\mathcal{C}_\tau =&(\tfrac{\bar a}{a})^2(1+w+v^{\boldsymbol{\cdot}})^2(\nu-1)\gamma_{x\phi}-\epsilon^2(1-\nu^2)\Big\{(1+w+v^{\boldsymbol{\cdot}})^2\Big(\chi_x+\nu\chi_\phi+\sqrt{\tfrac{\bar a}{a}}\nu\Big)[(1+2\gamma_x)\chi_{x\phi}-2\gamma_{x\phi}\chi_x]\\
&+\Big[2(1-\nu)(1+w+v^{\boldsymbol{\cdot}})^2\chi_{x\phi}+v'(1+w+v^{\boldsymbol{\cdot}})\Big(\chi_x+\nu\chi_\phi+\sqrt{\tfrac{\bar a}{a}}\nu\Big)\Big][(1+2\gamma_x)\chi_\phi-2\gamma_{x\phi}\chi_{x\phi}]\Big\}\ ,\\
\mathcal{D} =&\pm\,\epsilon^2(1-\nu^2)\Big\{(1+w+v^{\boldsymbol{\cdot}})^2\Big\{\sqrt{\tfrac{\bar a}{a}}[(1+2\gamma_\phi)(\gamma_\phi'-\nu\gamma_x'-2\gamma_{x\phi}^{\boldsymbol{\cdot}})+2\gamma_{x\phi}(\gamma_\phi^{\boldsymbol{\cdot}}-\nu\gamma_x^{\boldsymbol{\cdot}}+2\nu\gamma_{x\phi}')]\\
&+2(1-\nu)\chi_{x\phi}[(1+2\gamma_x)\gamma_\phi^{\boldsymbol{\cdot}}+2\gamma_{x\phi}(\gamma_\phi'-2\gamma_{x\phi}^{\boldsymbol{\cdot}})]+(\chi_x+\nu\chi_\phi)[(1+2\gamma_x)\gamma_\phi'-2\gamma_{x\phi}\gamma_x^{\boldsymbol{\cdot}}]\\
&+(\chi_\phi+\nu\chi_x)[(1+2\gamma_\phi)(\gamma_\phi'-2\gamma_{x\phi}^{\boldsymbol{\cdot}})+2\gamma_{x\phi}\gamma_\phi^{\boldsymbol{\cdot}}]-\tfrac{\bar a}{a}[\chi_x'+\nu\chi_\phi'+2(1-\nu)\chi_{x\phi}^{\boldsymbol{\cdot}}]\Big\}\\
&-\tfrac{\bar a}{a}\Big\{(1+w+v^{\boldsymbol{\cdot}})v'(\chi_x^{\boldsymbol{\cdot}}+\nu\chi_\phi^{\boldsymbol{\cdot}})+\Big(\chi_x+\nu\chi_\phi+\sqrt{\tfrac{\bar a}{a}}\nu\Big)[(1+w+v^{\boldsymbol{\cdot}})v'^{\boldsymbol{\cdot}}-v'(w^{\boldsymbol{\cdot}}+v^{\boldsymbol{\cdot\cdot}})]\Big\}\\
&+(1+w+v^{\boldsymbol{\cdot}})(\chi_x+\nu\chi_\phi)v'[(1+2\gamma_x)\gamma_\phi^{\boldsymbol{\cdot}}+(1+2\gamma_\phi)\gamma_x^{\boldsymbol{\cdot}}-4\gamma_{x\phi}\gamma_{x\phi}^{\boldsymbol{\cdot}}]+(\tfrac{\bar a}{a})^{\frac{3}{2}}(1+w+v^{\boldsymbol{\cdot}})^2c_x\Big\}\ ,\\
\mathcal{K} =&(\tfrac{\bar a}{a})^2\epsilon^2(1-\nu^2)(1+w+v^{\boldsymbol{\cdot}})^2\ .
\end{aligned}
\tag{A-14}
$$

Terms in (A-12) containing the external boundary moments are of the form

$$
\begin{aligned}
\mathcal{G}^*_\nu &= a_\tau^{-1}\epsilon^2(\nu^2-1)(1+w+v^{\bullet})[(1+2\gamma_\phi)\chi_{x\phi}-2\gamma_{x\phi}\chi_\phi]\Big[S\,M^*_\nu-\sqrt{\tfrac{\bar{a}}{a}}(1+w+v^{\bullet})M^*_\tau\Big]\ ,\\
\mathcal{G}^*_\tau &= a_\tau^{-1}\epsilon^2(1-\nu^2)(1+w+v^{\bullet})[(1+2\gamma_x)\chi_\phi-2\gamma_{x\phi}\chi_{x\phi}]\Big[S\,M^*_\nu-\sqrt{\tfrac{\bar{a}}{a}}(1+w+v^{\bullet})M^*_\tau\Big]\ ,\\
\mathcal{F}^*{}_{,s} &= \mp\,\epsilon^2(1-\nu^2)\Big\{(\tfrac{\bar{a}}{a})^{\frac{3}{2}}(1+w+v^{\bullet})^2(a_\tau^{-1}M^{*\bullet}_\tau-a_\tau^{-3}\gamma^{\bullet}_\phi M^*_\tau)+a_\tau^{-1}\tfrac{\bar{a}}{a}S\,[(w^{\bullet}+v^{\bullet\bullet})M^*_\nu-(1+w+v^{\bullet})M^{*\bullet}_\nu]\\
&\qquad -a_\tau^{-1}(1+w+v^{\bullet})\Big\{\tfrac{\bar{a}}{a}(S^{\bullet}-a_\tau^{-2}S\,\gamma^{\bullet}_\phi)-S\,[(1+2\gamma_\phi)\gamma^{\bullet}_x+(1+2\gamma_x)\gamma^{\bullet}_\phi-4\gamma_{x\phi}\gamma^{\bullet}_{x\phi}]\Big\}M^*_\nu\Big\}\ ,
\end{aligned}
\tag{A-15}
$$

where

$$
\begin{aligned}
S &= u^{\bullet}[v'u^{\bullet}-(1+u')(1+w+v^{\bullet})]-(v-w^{\bullet})[v'(w^{\bullet}-v)-w'(1+w+v^{\bullet})]\ ,\\
\tfrac{\bar{a}}{a} &= (1+2\gamma_\phi)(1+2\gamma_x)-4\gamma^2_{x\phi}\ ,\quad a_\tau = \sqrt{1+2\gamma_\phi}\ .
\end{aligned}
\tag{A-16}
$$

The BVP (A-10) to (A-16) describes the equilibrium prebuckling state of the finite cylinder. It is expressed in terms of the surface strain measures and modified curvatures as intermediate dependent functions. Please note that the upper (lower) signs in (A-10) to (A-15) correspond to $\partial\mathscr{M}_1$ ($\partial\mathscr{M}_2$).

The non-dimensional surface strains and modified curvatures are expressed in displacements by the exact kinematic relations

$$
\begin{aligned}
\gamma_\phi &= w+v^{\bullet}+\frac{1}{2}[u^{\bullet 2}+(w+v^{\bullet})^2+(w^{\bullet}-v)^2]\ ,\\
\gamma_{x\phi} &= \frac{1}{2}[u^{\bullet}+v'+u'u^{\bullet}+v'(w+v^{\bullet})+w'(w^{\bullet}-v)]\ ,\\
\gamma_x &= u'+\frac{1}{2}(u'^2+v'^2+w'^2)\ ,\\
\chi_\phi &= [(1+w+v^{\bullet})(1+u')-v'u^{\bullet}](w^{\bullet\bullet}-2v^{\bullet}-w-1)+[w'u^{\bullet}-(1+u')(w^{\bullet}-v)](v^{\bullet\bullet}+2w^{\bullet}-v)\\
&\quad +[v'(w^{\bullet}-v)-w'(1+w+v^{\bullet})]u^{\bullet\bullet}\ ,\\
\chi_{x\phi} &= [(1+w+v^{\bullet})(1+u')-v'u^{\bullet}](w'^{\bullet}-v')+[w'u^{\bullet}-(1+u')(w^{\bullet}-v)](w'+v'^{\bullet})\\
&\quad +[v'(w^{\bullet}-v)-w'(1+w+v^{\bullet})]u'^{\bullet}\ ,\\
\chi_x &= [(1+w+v^{\bullet})(1+u')-v'u^{\bullet}]w''+[w'u^{\bullet}-(1+u')(w^{\bullet}-v)]v''\\
&\quad +[v'(w^{\bullet}-v)-w'(1+w+v^{\bullet})]u''\ ,
\end{aligned}
\tag{A-17}
$$

which should be substituted into (A-10)-(A-15) in order to obtain the BVP expressed explicitly in terms of displacements. Unfortunately, such a displacement BVP is extremely complex and is available only in the computer memory, from which it can easily be made available, if necessary.

A.4. The membrane prebuckling state of axially compressed cylinder

In case of bifurcation buckling of the axially compressed circular cylindrical shell, only the axial force components parallel to the undeformed cylinder's generators is applied at its boundaries. Let us define this boundary force component by

$$N_\nu^* = -\frac{2\rho}{\epsilon} \; , \tag{A-18}$$

which compresses the cylinder when ρ takes positive values. The value $\rho = 1$ corresponds to the stress $\sigma_{cl} = 2\epsilon E h$. This value was first calculated by Lorenz (1911) by the linear stability theory of the axially compressed circular cylindrical shell with simply supported boundary conditions, see also Brush and Almroth (1975), Yamaki (1984). In this paper, we call $\rho = 1$ the classical value of the buckling load.

It is assumed that the axial compressive force causes contraction of the cylinder which is allowed to homogeneously expand in the radial direction. Such an assumption produces the following prebuckling equilibrium state for the axial u, circumferential v and radial w components of the displacement vector being the approximate solution of (A-10) to (A-17) with all external loads zero, except the force component N_ν^* given in (A-18):

$$\begin{aligned} u_0(\phi, x) &= Ux = [-2\epsilon\rho(1 + 3\epsilon\rho) + O(\epsilon^3)]x \; , \\ v_0(\phi, x) &= 0 \; , \\ w_0(\phi, x) &= W = 2\epsilon\nu\rho[1 + (2 - \nu)\epsilon\rho] + O(\epsilon^3) \; , \end{aligned} \tag{A-19}$$

where terms of the order $O(\epsilon^3)$ are omitted in the solution. The solution (A-19) satisfies exactly the first two equilibrium equations as well as the second and third static boundary conditions. The third equilibrium equation and the first static boundary condition are satisfied within the error $O(\epsilon^3)$. The remaining fourth static boundary condition is satisfied within the error $O(\epsilon)$. The first three geometric boundary conditions are satisfied because of free constants C_1, C_2, C_3. The remaining fourth geometric boundary condition is satisfied also because of free constant C_4, but in the derivation of incremental boundary conditions we have assumed $C_4 = 0$. Because all the non-equilibrated terms are of the order of error introduced by the constitutive equations (Opoka and Pietraszkiewicz, 2009, eq. (44)), the solution (A-19) can be considered as the quite accurate prebuckling equilibrium solution for the axially compressed cylinder satisfying static as well as geometric boundary conditions.

If we express the surface internal stress and moment resultants by the non-dimensional functions

$$
\begin{aligned}
&N_1^1 = \tfrac{D}{R^2} N_\phi(\phi, x) , \quad N_2^2 = \tfrac{D}{R^2} N_x(\phi, x) , \quad N_1^2 = R^2 N_2^1 = \tfrac{D}{R} N_{x\phi}(\phi, x) , \\
&M_1^1 = \tfrac{D}{R} M_\phi(\phi, x) , \quad M_2^2 = \tfrac{D}{R} M_x(\phi, x) , \quad M_1^2 = R^2 M_2^1 = D M_{x\phi}(\phi, x) ,
\end{aligned}
\tag{A-20}
$$

then for the equilibrium state (A-19) the surface stress and moment resultants obtained from the constitutive equations and the kinematic relations are

$$
\begin{aligned}
&N_\phi = O(1) , \quad N_{x\phi} = O(1) , \quad N_x = -\tfrac{2\rho}{\epsilon} + O(1) , \\
&M_\phi = O(\epsilon) , \quad M_{x\phi} = O(\epsilon) , \quad M_x = O(\epsilon) ,
\end{aligned}
\tag{A-21}
$$

where $O(1)$ and $O(\epsilon)$ are errors of the constitutive equations expressed in terms of the small parameter ϵ. Solution (A-21) describes, with accuracy up to unavoidable error in the constitutive equations, the membrane prebuckling state equivalent to the one used by Yamaki (1984) and in many other papers devoted to this problem.

A.5. Stability equations and corresponding incremental boundary conditions for the cylinder

The primary equilibrium state $\mathbf{u}_0$ being the solution of (A-10) to (A-15) may become unstable if an infinitesimally close adjacent equilibrium state $\mathbf{u}_1$ exists under the same system of external loads and boundary conditions. The loss of stability can be detected by the perturbation technique.

Let

$$
u_1 = u_0 + \mu u , \quad v_1 = v_0 + \mu v , \quad w_1 = w_0 + \mu w \tag{A-22}
$$

are values describing an adjacent equilibrium state, where now u, v, w are small increments of the basic displacement variables u_0, v_0, w_0 that occur at buckling, and μ is a small parameter. Introducing (A-22) into (A-10) and (A-12) expressed in displacements we can linearize the resulting equations with regard to the incremental fields and take into account that the fields u_0, v_0, w_0 satisfy the equilibrium BVP. Allowing no change in the applied loads at buckling, all linear terms in μ lead to the stability equations and incremental work–conjugate boundary conditions for the perfect cylinder. In order to perform this task we also have to transform the square roots of $\frac{\bar{a}}{a}$ to the equivalent forms; for example, the expression $(\frac{\bar{a}}{a})^{\frac{3}{2}}$ has been transformed to the form $\frac{\bar{a}}{a}\sqrt{\frac{\bar{a}}{a}}$, where $\frac{\bar{a}}{a}$ is represented exactly in strains, whereas $\sqrt{\frac{\bar{a}}{a}} \approx 1 + \gamma^{\alpha}_{\alpha}$. Finally, introducing (A-19) and rejecting terms which are of the order of error introduced by (A-19), we have obtained the following homogeneous stability equations for the axially compressed, perfect circular cylinder:

$$
\begin{aligned}
&A_1 w^{\bullet\bullet\bullet} + A_2 w^{\prime\prime\bullet} + A_3 u^{\prime\bullet} + A_4 v^{\prime\prime} + A_5 v^{\bullet\bullet} + A_6 w^{\bullet} = 0\ ,\\
&B_1(w^{\prime\bullet\bullet} + \nu w^{\prime\prime\prime}) + B_2 u^{\prime\prime} + B_3 u^{\bullet\bullet} + B_4[(1+\nu)v^{\prime\bullet} + 2\nu w^{\prime}] = 0\ ,\\
&C_1(w^{\prime\prime\prime\prime} + 2w^{\prime\prime\bullet\bullet} + w^{\bullet\bullet\bullet\bullet}) + C_2(u^{\prime\bullet\bullet} + \nu u^{\prime\prime\prime}) + C_3 v^{\prime\prime\bullet} + C_4 v^{\bullet\bullet\bullet} + C_5 w^{\prime\prime}\\
&\quad + C_6 w^{\bullet\bullet} + C_7 u^{\prime} + C_8 v^{\bullet} + C_9 w = 0\ ,
\end{aligned}
\qquad \text{(A-23)}
$$

with the corresponding sets of incremental work–conjugate boundary conditions

$$
\begin{aligned}
&D_1 w^{\prime\prime} + D_2 u^{\prime} + D_3(v^{\bullet} + w) = 0 && \text{or} \quad u = 0\ ,\\
&E_1 w^{\prime\bullet} + E_2 u^{\bullet} + E_3 v^{\prime} = 0 && \text{or} \quad v = 0\ ,\\
&F_1[w^{\prime\prime\prime} + (2-\nu)w^{\prime\bullet\bullet}] + F_2(u^{\bullet\bullet} + \nu u^{\prime\prime}) + F_3 v^{\prime\bullet} + F_4 w^{\prime} = 0 && \text{or} \quad w = 0\ ,\\
&G_1(w^{\prime\prime} + \nu w^{\bullet\bullet}) + G_2 v^{\bullet} + G_3 u^{\prime} + G_4 w = 0 && \text{or} \quad w^{\prime} = 0\ .
\end{aligned}
\qquad \text{(A-24)}
$$

The coefficients in (A-23) and (A-24) are defined as follows:

$$
\begin{aligned}
A_1 &= 4\epsilon^2(1-\nu^2)[1-\epsilon(2-5\nu)\rho-\epsilon^2(7+2\nu)\rho^2]+O(\epsilon^5)\ ,\\
A_2 &= 4\epsilon^2(1-\nu^2)[1-\epsilon(2-4\nu-\nu^2)\rho-\epsilon^2(6+\nu+2\nu^2)\rho^2]+O(\epsilon^5)\ ,\\
A_3 &= -(1+\nu)[1-2\epsilon(2-3\nu)\rho-2\epsilon^2(4+6\nu-3\nu^2)\rho^2]+O(\epsilon^3)\ ,\\
A_4 &= -(1-\nu)\{1-\epsilon(6-4\nu)\rho+2\epsilon^2[2(1-\nu^2)-(3+8\nu)\rho^2]\}+O(\epsilon^3)\ ,\\
A_5 &= -2\{1-2\epsilon(1-4\nu)\rho+2\epsilon^2[2(1-\nu^2)-(3-8\nu^2)\rho^2]\}+O(\epsilon^3)\ ,\\
A_6 &= -2\{1-2\epsilon(1-4\nu)\rho+2\epsilon^2[1-\nu^2-(3-8\nu^2)\rho^2]\}+O(\epsilon^3)\ ,\\
B_1 &= 4\epsilon^3(1-\nu^2)\rho[\nu-\epsilon(1+2\nu)\rho]+O(\epsilon^5)\ ,\\
B_2 &= -2[1-2\epsilon(5-\nu-\nu^2)\rho+2\epsilon^2(2-8\nu-3\nu^2+2\nu^3)]\rho^2]+O(\epsilon^3)\ ,\\
B_3 &= -(1-\nu)[1-2\epsilon(4-\nu)\rho-2\epsilon^2\nu(6+\nu)\rho^2]+O(\epsilon^3)\ ,\\
B_4 &= -1+\epsilon(6-4\nu)\rho+2\epsilon^2(3+8\nu)\rho^2+O(\epsilon^3)\ ,\\
C_1 &= -2\epsilon^2(1-\nu^2)[1-\epsilon(6-4\nu)\rho-2\epsilon^2(3+8\nu)\rho^2]+O(\epsilon^5)\ ,\\
C_2 &= 4\epsilon^3(1-\nu^2)\rho[\nu-\epsilon(1+4\nu-2\nu^2)\rho]+O(\epsilon^5)\ ,\\
C_3 &= 4\epsilon^2(1-\nu^2)[1-\epsilon[6-4\nu-\nu^2]\rho-\epsilon^2(6+17\nu+6\nu^2)\rho^2]+O(\epsilon^5)\ ,\\
C_4 &= 4\epsilon^2(1-\nu^2)[1-\epsilon(6-5\nu)\rho-\epsilon^2(7+22\nu)\rho^2]+O(\epsilon^5)\ ,\\
C_5 &= -4\epsilon(1-\nu^2)[\rho-\epsilon(\nu+4(1-\nu)\rho^2)]+O(\epsilon^3)\ ,\\
C_6 &= 4\epsilon^2(1-\nu^2)+O(\epsilon^3)\ ,\\
C_7 &= -2\nu[1-2\epsilon(4-3\nu)\rho-6\epsilon^2(6-\nu)\nu\rho^2]+O(\epsilon^3)\ ,\\
C_8 &= -2[1-2\epsilon(3-4\nu)\rho+2\epsilon^2(1-\nu^2-(3+16\nu-8\nu^2)\rho^2)]+O(\epsilon^3)\ ,\\
C_9 &= -2[1-2\epsilon(3-4\nu)\rho+\epsilon^2(1-\nu^2-2(3+16\nu-8\nu^2)\rho^2)]+O(\epsilon^3)\ ,
\end{aligned}
\tag{A-25}
$$

and

$$
\begin{aligned}
D_1 &= -4\epsilon^3\nu(1-\nu^2)\rho[\nu-\epsilon(1+2\nu)\rho]+O(\epsilon^5)\ ,\\
D_2 &= 2[1-2\epsilon(5-\nu-\nu^2)\rho+2\epsilon^2(2-8\nu-3\nu^2+2\nu^3)\rho^2]+O(\epsilon^3)\ ,\\
D_3 &= 2\nu[1-\epsilon(6-4\nu)\rho-2\epsilon^2(3+8\nu)\rho^2]+O(\epsilon^3)\ ,\\
E_1 &= 4\epsilon^2(1-\nu^2)[1-\nu-\epsilon(2-6\nu+3\nu^2)\rho-\epsilon^2(6-5\nu+2\nu^2)\rho^2]+O(\epsilon^5)\ ,\\
E_2 &= -(1-\nu)[1-2\epsilon(2-3\nu)\rho-2\epsilon^2(4+6\nu-3\nu^2)\rho^2]+O(\epsilon^3)\ ,\\
E_3 &= -(1-\nu)[1-\epsilon(6-4\nu)\rho+\epsilon^2(4-4\nu^2-6\rho^2-16\nu\rho^2)]+O(\epsilon^3)\ ,\\
F_1 &= -2\epsilon^2(1-\nu^2)[1-\epsilon(6-4\nu)\rho-2\epsilon^2(3+8\nu)\rho^2]+O(\epsilon^5)\ ,\\
F_2 &= 4\epsilon^3(1-\nu^2)\rho[\nu-\epsilon(1+4\nu-2\nu^2)\rho]+O(\epsilon^5)\ ,\\
F_3 &= 4\epsilon^2(1-\nu^2)[1-\epsilon(6-4\nu-\nu^2)\rho-\epsilon^2(6+17\nu+6\nu^2)\rho^2]+O(\epsilon^5)\ ,\\
F_4 &= -2\epsilon(1-\nu^2)[2\rho-\epsilon(\nu+8(1-\nu)\rho^2)]+O(\epsilon^3)\ ,\\
G_1 &= -1+2\epsilon(1-\nu)\rho+2\epsilon^2(3+\nu^2)\rho^2+O(\epsilon^3)\ ,\\
G_2 &= 2\nu[1-\epsilon(3-2\nu)\rho-\epsilon^2(9+2\nu+2\nu^2)\rho^2]+O(\epsilon^3)\ ,\\
G_3 &= 2\epsilon\nu\rho[1+2\nu+\epsilon(3+4\nu)\rho]+O(\epsilon^3)\ ,\\
G_4 &= \nu[1-2\epsilon(2-\nu)\rho-2\epsilon^2(6+2\nu+\nu^2)\rho^2]+O(\epsilon^3)\ .
\end{aligned}
\tag{A-26}
$$

where the terms $O(\epsilon^k)$ at the end of each line are omitted because they all fall into the error introduced by the approximate prebuckling solution (A-19).

If we substitute the prebuckling solution $u_0(\phi, x) = Ux,\ v_0(\phi, x) = 0,\ w_0(\phi, x) = W$ into the general stability problem containing u_0, v_0, w_0 and u, v, w then the coefficients A_i, B_i, C_i in (A-25) and D_i, E_i, F_i, G_i in (A-26) are not all equal zero. If we assume (A-19) to contain only the principal terms of the order $O(\epsilon)$, the coefficient C_6 falls into the error order of the approximate prebuckling solution and the term $C_6 w^{\cdot\cdot}$ in (A-23) disappears, which can lead to inaccurate results. Therefore, in derivation (A-23)–(A-26) we have used the prebuckling state (A-19) in which the principal terms $O(\epsilon)$ as well as the secondary terms $O(\epsilon^2)$ must have been taken into account. Including tertiary terms $O(\epsilon^3)$ in (A-19) takes no effect on the value of buckling load for the axially compressed cylinder with clamped boundary condition C1 and, thus, such tertiary terms are not considered in (A-19).

Repeating the above procedure for the simplified BVP, in which only the underlined terms are taken into account (Opoka and Pietraszkiewicz, 2009, eq. (21)), and using the same prebuckling state (A-19) (the corresponding prebuckling states differ in tertriary order terms), the following simplified stability equations are obtained

$$
\begin{aligned}
&A_1 u'^{\bullet} + A_2[2w^{\bullet} + 2v^{\bullet\bullet} + (1-\nu)v''] = 0 \;, \\
&B_1[(1-\nu)u^{\bullet\bullet} + 2u''] + A_2[(1+\nu)v'^{\bullet} + 2\nu w'] = 0 \;, \\
&C_1(w^{\bullet\bullet\bullet\bullet} + 2w''^{\bullet\bullet} + w'''' - 2v''^{\bullet} - 2v^{\bullet\bullet\bullet}) + C_2 w'' + C_3 w^{\bullet\bullet} + C_4 u' + C_5(v^{\bullet} + w) = 0,
\end{aligned}
\tag{A-27}
$$

where

$$
\begin{aligned}
A_1 &= (1+\nu)(1 - 2\epsilon\rho - 6\epsilon^2\rho^2) + O(\epsilon^3) \;, \\
A_2 &= 1 + 2\epsilon\nu\rho + 2\epsilon^2(2-\nu)\nu\rho^2 + O(\epsilon^3) \;, \\
B_1 &= 1 - 2\epsilon\rho - 6\epsilon^2\rho^2 + O(\epsilon^3) \;, \\
C_1 &= \epsilon^2(1-\nu^2)(1 - 2\epsilon\rho - 6\epsilon^2\rho^2) + O(\epsilon^5) \;, \\
C_2 &= \epsilon(1-\nu^2)(2\rho - \epsilon\nu) + O(\epsilon^3) \;, \\
C_3 &= -\epsilon^2(1-\nu^2) + O(\epsilon^3) \;, \\
C_4 &= \nu[1 - 2\epsilon(2-\nu)\rho - 2\epsilon^2(4 + 2\nu + \nu^2)\rho^2] + O(\epsilon^3) \;, \\
C_5 &= 1 - \epsilon(2 - 4\nu)\rho - 6\epsilon^2\rho^2 + O(\epsilon^3) \;.
\end{aligned}
\tag{A-28}
$$

The corresponding simplified static boundary conditions are not relevant for the case of clamped boundary considered in the main body of this paper and therefore they are not provided here.

The BVP (A-10) and (A-12) as well as the kinematic relations (A-17) and the general stability problem have been automatically generated using the package *ShellBVP.m*.